AALTO UNIVERSITY
School of Science and Technology
Department of Surveying

Chen Xiaojie

Spatial Modeling and Simulation of the Common Reed in the Gulf of Finland

AALTO UNIVERSITY

School of Science and Technology

Degree Programme of Surveying Department

ABSTRACT OF
MASTER'S THESIS

Author: Chen Xiaojie	
Title of thesis:	
Spatial Modeling and Simulation of	
the Common Reed in the Gulf of Finland	

Date:	May 26th, 2010	**Pages:** 88

Professorship: Department of Civil and Environmental Engineering
Code: Maa-123 Geoinformatics

Supervisor:	Professor Ari Jolma
Instructor:	M.Sc. Anas Altartouri

Invasive species have been recognized globally as a major environmental problem. *Phragimites australis*, the common reed, is rapidly expanding on the Finnish coast of the Gulf of Finland, lowering its property value and causing ecological consequences. This invasive expansion can be controlled by strategic management plans. Hence, the present study introduces a model capable of simulating the expansion of *Phragimites australis* in order to serve as a tool for environmental management. This research approaches the matter by firstly providing a method for delineating the common reed coverage from LiDAR data. Secondly, factors explaining the phenomenon are proposed, analyzed, and aggregated, providing transitional rules for the cellular automata model. Finally, a cellular automata model is developed to simulate the dynamic of this phenomenon and build scenarios of possible future coverage of *Phragimites australis* in the study area. The results demonstrate successful model functionality for producing scenarios of the common reed expansion. The study indicates also the potential of combining cellular automata and GIS technology to model the expansion of invasive species and provide useful management tool.

Keywords:	Cellular automata; Common reed; GIS; LiDAR; Modeling; *Phragmites australis*; Simulation;
Language:	English

Acknowledgements

Contents

List of Figures

List of Tables

Listings

Abbreviations

CA	Cellular Automata
DDM	Digital Depth Model
DEM	Digital Elevation Model
DSM	Digital Surface Model
DSS	Environment Decision Support System
GIS	Geographic Information System
GPS	Global Positioning System
GRASS	Geographic Resources Analysis Support System
GUI	Graphical User Interface
LiDAR	Light Detection And Ranging
ND	Normal Distribution
SD	Standard Deviation
TIFF	Tagged Image File Format
UTM	Universal Transverse Mercator

Chapter 1

Introduction

1.1 Rationale

Invasive species are one of the top drivers for global environment problem increasing as a consequence of tourism and globalization [Mooney et al., 2005]. Invasive species can change the functions of ecosystems, invasive plants can alter the fire regime, nutrient cycling and hydrology in native ecosystems [Mack et al., 2000].As a widespread and aggressive invasive species, *Phragmites australis* (hereafter *Phragmites* or common reed), has increased dramatically in distribution and abundance [Rickey and Anderson, 2004]. This invasive species appears to be nearly global in distribution in fresh and brackish waters, it affects the landscape, hydrology and drainage density [Weinstein and Balletto, 1999], thus causes serious threat to the local ecosystems.

In Europe, during the 1990s, *Phragmites* attracted attention in several European countries [van der Putten, 1998]. In Finland, the common reed has spread extensively in the inner and middle archipelago areas in the Gulf of Finland, now covering up to 8% along the southern coastal area [Pitkanen, 2006]. This invasive phenomenon of Phragmites australis is linked to several environmental concerns including invasive species, habitat change and biodiversity loss as well as nutrient overloading [Gewin, 2005]. Therefore, effective control or even eradication is needed repeatedly for such invasive species[Mack and Lonsdale, 2002].

As in major invasive plant control issue, a considerable return for limited resources rests in prioritization of sites, monitoring, early discovery and removal, as well as vigilance thereafter [Staffen et al., 2003]. One effective mean

for controlling invasive species is to monitor susceptible areas and destroy the new plants before expansion [Staffen et al., 2003]. Monitoring susceptible area would also allow quantifying the consequences resulting from the expansion and define more sensitive area for well-informed decision making and effective management measures. Hence, there is a need for developing a simulation model which predicts the spread of *Phragmites australis*.

This research addresses the phenomenon of the *Phragmites* spread in the Gulf of Finland. This phenomena of *Phragmites* spreading can be fit into Geographic Information System (GIS) environment. Moreover, spatial analysis approach, modeling method and plant expansion simulation can be combined and supported by GIS. The growing simulation can provide adequate result for further analysis and management. Besides, visual simulation can assist in building a Environmental Decision Support System (EDSS) which can facilitate management and decision making process.

1.2 Aim and objectives

The aim of this research is to develop a simulation model of the expansion of *Phragmites australis* in the Finnish coast of the Gulf of Finland. This simulation model can provide visual and statistical results which represent *Phragmites australis* expansion area during a predefined period of time.

In order to achieve the aim, several objectives must be met:

- Mapping of the common reed coverage by processing LiDAR data.

- Investigation of the environmental factors associated with the existence and expansion of common reed. This includes comprehensive revision of common reed ecology and statistical testing of these factors' relevance to the phenomenon.

- Testing the potential aggregation methods by which explanatory factors can be expressed in a succinct manner.

- Development of a cellular automata (CA) simulation model based on well-defined plant expansion rules.

1.3   Research design

The research approaches the objectives through four phases (see Figure 1.1). In the first phase, literature review is conducted in order to understand deeply the problems in question, i.e. nature of the reed expansion phenomenon, methods to be used, data to be acquired. Then, the study moves to the second phase where LiDAR data is analyzed and processed, resulting in extraction of the common reed coverage. Moving to the third phase, where the CA simulation model is developed. This phase consists of four steps: common reed growing and expansion phenomenon analysis; determination of weighted factors concerned with the phenomenon; choose a suitable method for aggregating those factors; and development of CA simulation model. Finalized by simulation outcome analysis and model calibration, the results of the model are discussed and conclusions are drawn in phase 4.
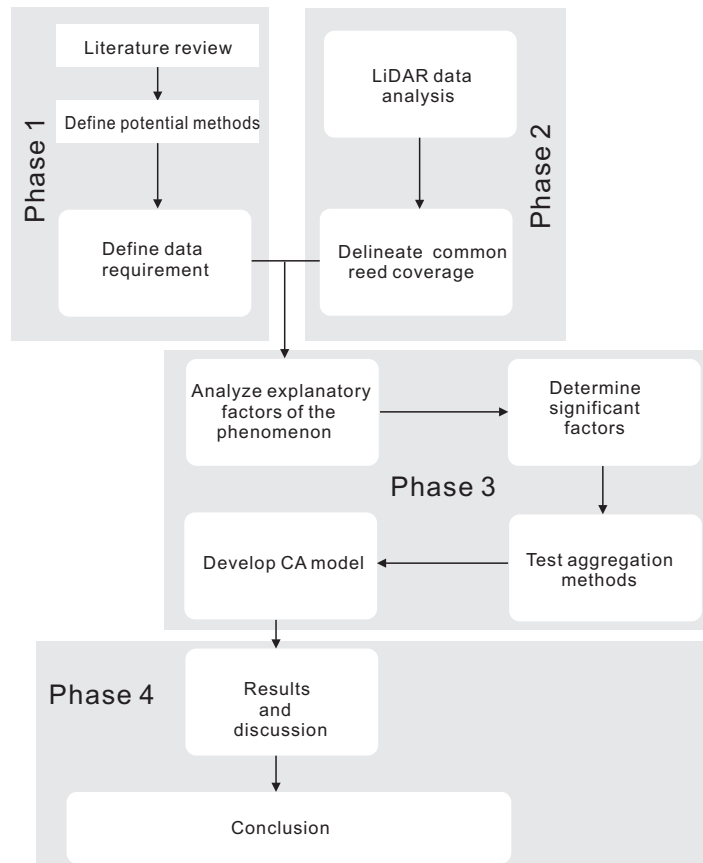
Figure 1.1: Research design in 4 phrases

1.4   Research context

This research was carried out within the frame of project IBAM(Integrated Bayesian risk Analysis of ecosystem Management in Gulf of Finland). The model integrates risk management of five themes: fisheries, eutrophication, oil spills, dioxin risks related to the consumption of herring, and climate change. *Phragmites* existence and expansion status are linked with five themes in different scales.

1.5   Contents of the thesis

This section describes the abstracts of each chapter in the paper; it gives guidance for reading of different level of readers. This paper is elaborated in seven chapters:

Chapter 1 introduces research context, objectives and research design.

Chapter 2 includes literature review, theory analysis and previous work associated with current research.

Chapter 3 describes the study area and materials.

Chapter 4 explains the data processing method and determines influential factors concerned with plant growing.

Chapter 5 studies cellular automata methodology in Geoscience and explains the simulation model implementation.

Chapter 6 analyzes different scenario of the simulation model.

Chapter 7 concludes and finalizes this research by given further recommendation for the simulation model.

Chapter 2

State of Art

This chapter provides background information for the common reed, explanatory factors of common reed expansion phenomenon, mapping methods for common reed, and cellular automata simulation theory.

2.1 The common reed

Phragmites australis, the common reed, is a large perennial grass found in wetlands throughout temperate and tropical regions of the world [Saltonstall, 2006]. The plant commonly forms extensive stands (known as reed beds usually 100-300 shoots per 1 m^2), which can occupy as much as a square kilometer or more in extent and be capable of fast spreading when conditions are favorable. As an aggressive species, common reed can spread both vegetatively with rhizomes and with seeds [Gucker, 2010]. Reproduction by seeds is poor, and most of the spreading happens with rhizomes [Haslam, 1972; Bart and Hartman, 2003]. It requires neutral or alkaline water conditions [Bart and Hartman, 2003], and does not usually occur where the water is acidic. It tolerates brackish water, and is often found at the upper edges of estuaries and on other wetlands which are occasionally inundated by the sea [Havens et al., 2003].

The common reed invasion may be having deleterious effects on fish populations and possibly on predators that prey upon them. The reed has been demonstrated to have a negative effect on larval and small juvenile fish, but less or no effect on larger fish [Able and Hagan, 2000, 2003]. Reed beds may be inadequate larval habitats and prey availability is decreased because of less diverse invertebrate taxa [Raichel et al., 2003]. In other words, common

reed beds can be important habitats for aquatic invertebrates, insects and several bird species [Ikonen and Hagelberg, 2007].

2.2 Explanatory factors of common reed expansion

The phenomenon of *Phragmites australis* expansion is dramatic and noteworthy in the Gulf of Finland. To assess the determinants of the common reed expansion, this research examines the spatial tolerance, ecological constrains and competitive abilities of common reed. The determinants of the species expansion consider the ability to establish new colonies and to increase existing colonies. Establishment and expansion can be considered as propagate dispersal, establishment then growth, expansion and creation of new generations (see Figure 2.1). Environmental factors concerned with plant growth, fecundity, and survival vary greatly across the range of habitants suitable for *Phragmites australis*.

In a typical coastal area, explanatory factors contributing to plant expansion include water depth, shading, sediment and wrack deposition, freezing peroid, wave and ice erosion, drought, and nutrient limitation [Burdick and Konisky, 2003].
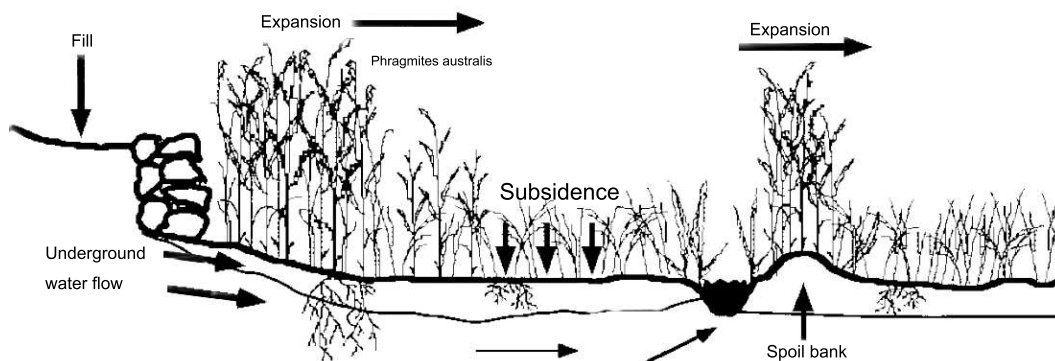
Figure 2.1: Common reed expansion process

Determination factors are categorized into three classes: ecological factors which explain the chief environmental factors governing distribution of reed expansion, including salinity, water depth, sediment type, nutrient level, and

interaction with other organisms; spatial factors which study entities of topological, geometric, and geographic properties, including elevation, slope, and topography; human factors which explains the way humans relate to the world, for instance constructions along coastal area, seashore conservation, pollution and activities related to common reed expansion. These group of factors are discussed in following paragraphs.

2.2.1 Ecological factors

The reed beds have several competitive advantages against other plants, which makes the aggressive spreading possible. Tall and dense reed beds prevent light penetration and suppress other species. Decomposing reed mat also covers the ground and inhibits other species growth, so once the reed stands appear to a place, it is very difficult for other species to compete with reed. The global spread can be explained with the high tolerance of reed to different environmental conditions. The reed is a robust competitor in several ways [Burdick and Konisky, 2003]. It prefers nutrient-rich habitats, and thus eutrophication can be one explanation for the reed expansion. The reed can grow in lakes and brackish water, and tolerance to changes in salinity is high. The reed also stands a lot of variation in soil pH (3.6-8.6), and has a wide tolerance to water level fluctuations [Lelong et al., 2007; Hayball and Pearce, 2004].

Occasionally reed beds may diminish or collapse. Factors causing decrease in reed beds are extreme water levels during winter together with low temperatures, strong ice activity, strong waves and wind and serious drought during the vegetative period [R.Bodensteiner and O.Gabriel, 2003; E. Minchinton, 2002]. Grazing used to be a strong controlling factor when agriculture was strong everywhere. This has been shown in simulated grazing tests [Hayball and Pearce, 2004], and the heavy urbanization in last decades may have accelerated the spread of reed due to decreased grazing.

2.2.2 Spatial factors

Spatial explanatory factors cover elevation, slope, aspect, hill-shape, archipelago distribution, sea openness (explained in Chapter 4), river mouths proximity and the other potential elements affect common reed expansion. Elevation and slope appear to be 2 influential factors. Common reed establishment is restricted to muddy sites (soft sea bottom) with proper water level [Doody et al., 2007]. *Phragmites australis* species growing across a range

of elevations: low, below mean high water; mid, around mean high water; high, above mean high water [Burdick and Konisky, 2003].

Common reed establishment is restricted to muddy sites and soft sea bottom with proper water level [Doody et al., 2007]. High water levels can drown the plant, and lack of water leads to desiccation. Field sites suitable for reed emergence are typically unflooded and unshaded. The common reed habitat type occurs on seasonally flooded sites where water ranges from 20 cm to 1 m below the soil surface. Fluctuating water levels are also tolerated by common reed [Hall, James B.; Hansen, Paul L. 1997].

Distance to river mouths affects the expansion process in the mean of organic sediments. Organic matter in the shelf sediments is mainly of marine origin, with increasing terrigenous components only close to rivers and estuaries [Alt-Eppinga et al., 2007]. Common reed occupies a wide variety of substrates and tolerates a range of organic matter, nutrients and pH levels [Gucker, 2010; Lee Ellis, 2005]. The establishment, expansion and ecosystem effects of *Phragmites australis* described it as an "ecosystem engineer" after finding that true elevation, peat accumulation, and organic matter increased while sediment bulk density decreased with increased common reed dominance. Not consistently demonstrated over all sites, however, sediment properties have impacts on common reed growth [Gucker, 2010].

Phragmites australis is most common in full sun or nearly full sun conditions [Jepson and Hickman, 1993]. A review reports that common reed height and density are lower in partially shaded areas [Kiviat and Hamilton, 2001]. As regards to the Finish coast of the Gulf of Finland, the hill-shade attribute has a limited impact on the common reed growth due to the flat nature of the area and, thus, can be neglected.

2.2.3   Human factors

Human impacts provide a partial explanation of how *Phragmites* expands and competes so well. Hydrological alterations, construction activities, and lowered salinity can explain the spread of reed [Bart and Hartman, 2003; Burdick and Konisky, 2003; Havens et al., 2003]. There is evidence that variations in climatic conditions, particularly increased precipitation enhance the performance of *Phragmites* [E. Minchinton, 2002]. The increasing CO_2 in atmosphere also favours the reed over some other competing species [Burdick and Konisky, 2003].

Different land-use may also cause a shift from native dominating genotype to another invasive genotype [Lelong et al., 2007]. There are differences in

ability to expand with different genotypes of the reed. Native and invasive *Phragmites* species both respond positively to increased nutrients, but human introduced plants clearly outperform natives, growing taller, producing more stems, and having higher biomass [Saltonstall and Stevensona, 2007].

2.3   Mapping of common reed

As an invasive species, previous work of mapping similar plant utilizes remote sensing technologies. Remote sensing images have gained success in providing spatial information on land cover characteristics to land managers that increase effective management of invasions into native habitats [Underwood et al., 2003]. In contrast to field-based surveys, imagery can be acquired for all habitats, over a much larger spatial area, and in a short period of time. The wealth of spectral information provided by hyper-spectral sensors allows for the species-level detection necessary to map invasive herbaceous species [Clarka et al., 2005].

However, most of the plants are spectrally similar because they are composed of the same spectrally active materials: pigments, water, cellulose, etc. [Jacquemoud and Baret, 1990]. Similarities among different species interfere the mapping and classification for invasive species. Moreover, the accuracy of mapping results decreases, since the spectral uniqueness is requisite for hyper-spectral detection [Andrew and Ustina, 2008]. Thus, there is a need for new methods of mapping the common reed which overcomes the problems associated with the hyper-spectral-based method.

Light Detection and Ranging provides high resolution horizontal and vertical spatial point cloud data, and is increasingly being used in a number of applications and disciplines, which have concentrated on the exploit and manipulation of the data using its three dimensional nature [Antonarakis et al., 2008]. In order to classify *Phragmites australis*, elevation and intensity LiDAR data are used in this study. Mapping and classification recently have been attempted with multi-spectral imagery [Duda et al., 1999; Sun et al., 2003], as a new type of remote sensing data LiDAR has the advantage of being able to create elevation surfaces such as digital elevation model (DEM) and digital surface model (DSM), while contain information on LiDAR intensity values, it is a spatial and spectral segmentation combined data source.

Classifications by using LiDAR have been attempted to derive several land features. In the study of Brennan and Webster [2006], they use attributes including mean intensity, Normal Height, Digital Surface Model, and Mul-

tiple Waveform LiDAR return to classify among 10 land features. LiDAR based classification have also been used by Charaniya et al. [2004], in their study, point cloud elevation and intensity data were applied to classify roofs, grass, trees, and roads. With assistance of spectral bands image, Bartels and Wei [2006] extract land types of buildings, vegetations, and ground in urban area.

In this study, however, the common reed is the only interesting class to be extracted. The distribution characteristics of the common reed explained in Section 2.2 need to be understood beforehand in order to develop appropriate LiDAR classification models. Classification models can be defined as the way to derive desired feature classes, the common reed in this study. Preliminary, the height and intensity attributes can be used in the classification of the common reed from LiDAR point cloud. The classification results is a map of the common reed in study area. The implementation of LiDAR classification methods of LiDAR will be explained in Section 4.1.

2.4 Cellular automata simulation theory

A cellular automaton (CA) is a discrete model studied in computability theory, mathematics, physics, theoretical biology and micro-structure modeling. It consists of a lattice of sites, each with a finite set of possible values. The values of the sites evolve synchronously in discrete time steps according to identical rules. The value of a particular site is determined by the previous values of a neighborhood of sites around it [Wolfram, 1984]. Although the approach of cellular automata is decades old, its widespread development and acceptance across the natural sciences has been relatively recent and is rapidly accelerating, and may become the archetypal description for certain kinds of systems [Fonstad, 2006].

2.4.1 Introduction to cellular automata

John Conway's "Game of Life" was the first well known application of cellular automata [Gardner, 1970]. Range of spatio-temporal dynamics allowed in the simple CA models is similar to range of allowed dynamics in the continuum description of the universe [Toffolia, 1984].

CA began to be used as a simulation world-view in Geosciences. The idea of "cellular geography" was introduced by Tobler[1979], he presents the idea that several distributed geographical concepts could be simulated by CA models.

Tobler [1980] introduced his idea to urban growth and land cover change based on CA. CA contains important capabilities in developing simulation models, and cellular automata simulations are gaining increased attention and being widely used in Geoscience.

Current research of CA in Geosciences focuses on several disciplines: transition rules developing; finding suitable computing environment including programming language, data structure, and hardware implementation; integration of other fields including statistical method, expert system and multi-agent system; simulation result validation. Those criteria are crucial in development of cellular automata models in geosciences model, in our case the model refers to common reed expanding simulation.

2.4.2   Components of CA model

Although the application fields vary in great ranges, cellular automata modeling share certain similarities. Generally, cellular automata consist of five ingredients: universal environment, cell states, cell neighborhoods, transition rule and edge effect. These will be discussed in the following paragraphs.

Universal environment

The universal environment defines cellular automaton structure during the computation process. Structures with discrete boundaries may be formed from continuous models [Wolfram, 1986]. CA model can be computed in 1 dimension, 2 dimensions (2D) and 3 dimensions (3D) [Jarvis et al., 2000], illustrated respectively in Figure 2.2, Figure 2.3 and Figure 2.4.
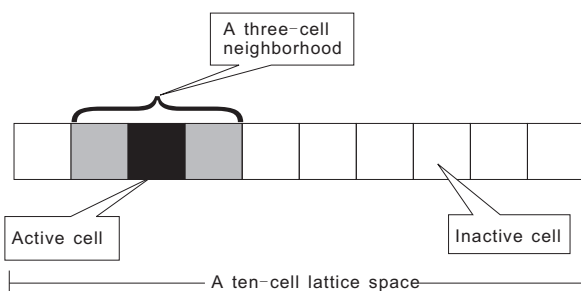
Figure 2.2: One-dimensional CA model

A widely used structure in the field of Geoscience is 2D, which consists of a discrete lattice of cells formed by triangle, rectangle, hexagon, or other
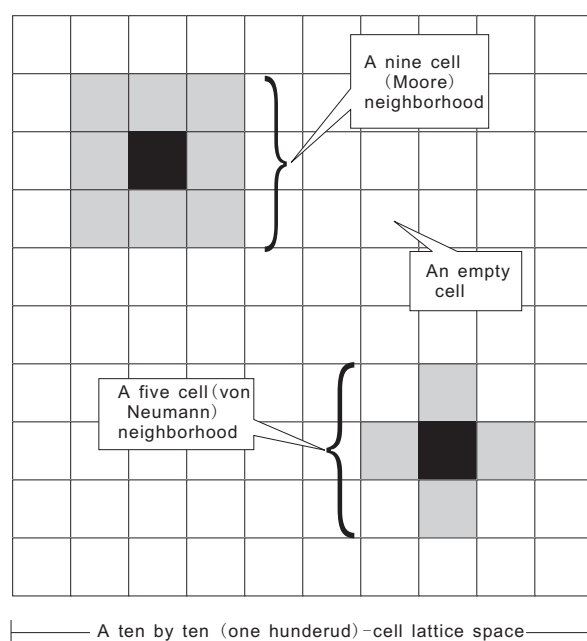
Figure 2.3: Two-dimensional CA model
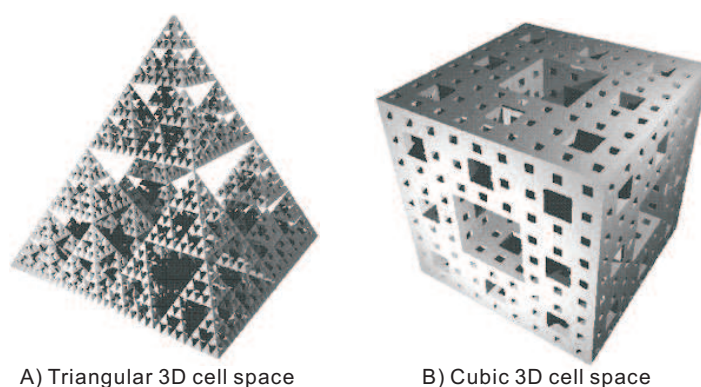
Figure 2.4: Three-dimensional CA model

topology [Goodchild, 2006] (see Figure 2.5). The assumption of cellular automata models is CA lattice is computed in a Euclidean space. Among several universal environments, the simplicity of the square-lattice approach and its similarity to the raster spatial data in Geoscience make it the basis for further development [Fonstad, 2006].

A)Triangle cell   B) Rectangle cell   C) Hexagon cell
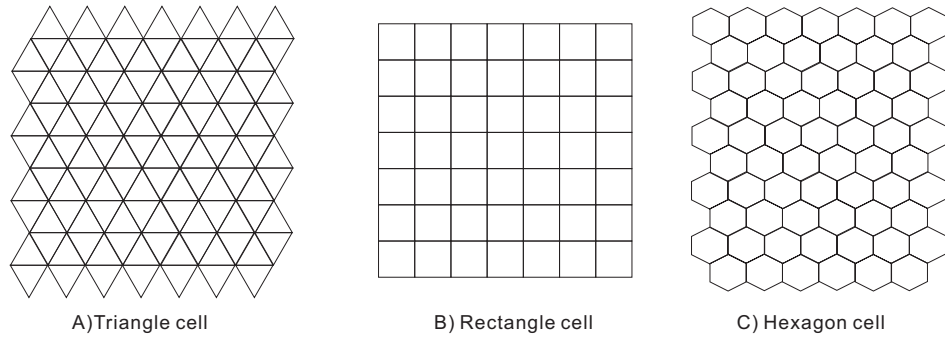
Figure 2.5: Triangular, rectangle, and hexagon lattices

Cell neighbourhoods

Two-dimensional lattice gives several possibilities for cell neighbourhood formation. For instance, von Neumann neighborhood (Figure 2.6 A) defines a cell with four neighboring cells in four directions: south, north, east, and west. Differently, Moore neighborhood (Figure 2.6 B) defines eight neighboring cells around each cell with the extra directions including south-west, north-west, south-east and north-east. Two types of neighborhoods above mentioned can be treated as radius 1 neighborhood, Figure 2.6 C illustrates the neighborhood type with radius 2.

A) 4 neighborhoods(vonNeumann)   B) 8 neighborhoods (Moore)   C) 8 neighborhoods with radius 2
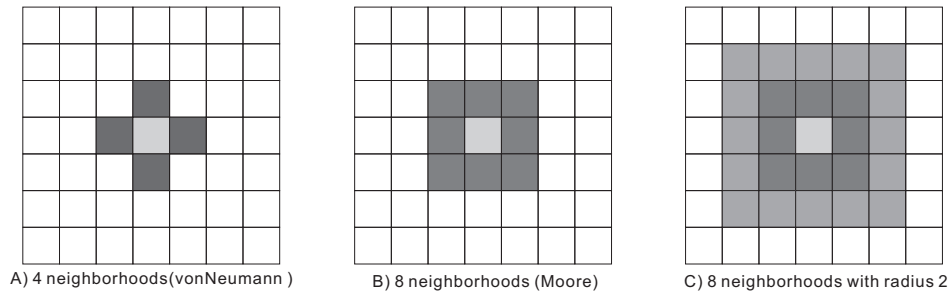
Figure 2.6: von Neumann and Moore neighborhood

Cell states

Each cell in the CA model can have finite number of states [Yacoubi and Jai, 2002]. The simplest set of states a cell can have is defined as "on" and "off", respectively computed as "1" and "0" in CA applications. For example, in

Figure 2.3, "active cells " (represented in black) can be compared to state
"1" and "empty cells" refer to state "0". More specifically, in common reed
case, the cell state can be simplified as "reed-occupied" (denoted as "1") and
"reed-free" (denoted as "0").

An initial state is created configured before the program start, which can
be seen as iteration 0, and cell generation 0. A new generation is created
(iteration=1), according to well defined rules that determine the new state of
each cell in terms of its current state and the current states of its neighbouring
cells [Wolfram, 1984]. For example, in this study, the rule might be defined
such as a cell can become "reed-occupied" (reed expands into it) only if three
of its defined neighbours were "reed-occupied", otherwise the cell does not
change its state (i.e. reed does not expand into it). CA rules used for
updating the cell states are fixed without changing as the program is running,
and are applied on the grid universe without an exception [Toffolia, 1984].

Transition rules

Transition rules, generally treated as mathematical functions, control the
change in the states of cells in discrete time steps (iterations) [Wolfram,
2002]. CA transition rules are applied in parallel on every cell in the grid en-
vironment. The rules do not change as the discrete time, or iteration changes
while computing. Individually, rules applied on a cell can be deterministic
or stochastic. Those two characteristics have opposite abilities: determinis-
tic rules applied on cell and require every cell in one iteration present the
same probability; stochastic allow different probabilistic cell exist in the same
cellular automata iteration [Colasanti et al., 2007; Fonstad, 2006].

CA models vary in the concept of deterministic and stochastic [Fonstad,
2006]. Iterations are completed after applying the transition rules to all
cells in the universal grid environment [Wolfram, 1986, 1984]. Normally,
next iteration computing is based on the current generation. Particularly,
cellular automata can run backwards, if it is possible, this give it attribute
of reversible [Fonstad, 2006]. However, if the cell states can not computed as
backwards, CA model will be treated as irreversible, and the simulation can
only be forwarded [Bolliger et al., 2003; Kronholm and Birkeland, 2004].

There is no fixed and clear answer for defining the transition rules. Transi-
tion rules might come from expert opinion in related fields. Rules can also
be generated from data analysis, but commonly rules are derived from com-
bination of sources. For instance, in the common reed expansion case, rules
are partly derived from the analysis of the reed coverage at specific years of

the past decades.

Chapter 3

Study Area and Materials

3.1 Study area

This research is carried out on the Finnish coast of the Gulf of Finland, (latitude of 60°00' N and longitude of 27°00' E). Major part of the area is located in UTM (Universal Transverse Mercator) zone $34v$ and $35v$. The study area is considered as an island-rich archipelago. The coastline of the area is complex, with a total shore length of about 8200 km. The mean water depth of the Gulf of Finland is 38 meters [Zhang et al., 2005] and shallower in the study area. The location of the research area is illustrated in Figure 3.1.

The methods and simulation model implemented in the study are are applied specifically on two sites within the study area. The first study site is located in Otaniemi promontory (60°10'30" - 60°11'30" N latitude, 24°48'30" - 24°50'30" E longitude). On this site, the method of extracting the common reed coverage out of the LiDAR data is applied.

The second site is located near Porvoo city and River Porvoo outlet in the Gulf of Finland. On this site, the developed CA simulation model was experimented. The site was chosen due to the influence of River Porvoo (Porvoonjoki in Finnish); the river brings massive amount of substances to the site which subsequently creates suitable conditions for the expansion of *Phragmites*. Figure 3.2 illustrates the location of both sites within the study area.

Figure 3.1: Location of the study area

3.2 Datasets

Datasets used in this study are categorized into three types: Light Detection
And Ranging (LiDAR)data, raster data, and vector data. These datasets are
enumerated and discussed in the following subheadings.

Figure 3.2: Location Otaniemi bay and study site in Porvoo

3.2.1 LiDAR data

The airborne laser scanning data, LiDAR, provides high-resolution point cloud (see Figure 3.3) and has been applied recently in the characterization, quantification and monitoring of coastal environments. LAS viewer is used for displaying the LIDAR point cloud data. Figure 3.3 illustrates a LiDAR

point cloud near Otaniemi area (60°11'21" N, 24°50'8" E), the cloud is displayed in LAS Viewer, a software for displaying LiDAR data.
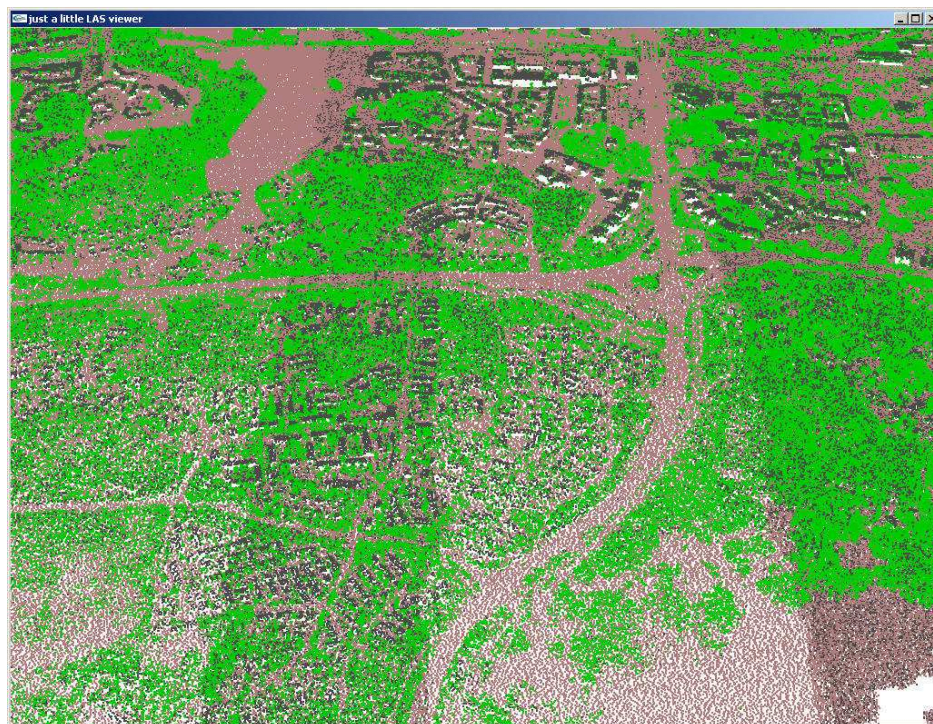
Figure 3.3: LiDAR point cloud displayed in LAS viewer

This research employs LiDAR data to delineate the coastal area dominated by the common reed in the first study site. Several types of data layers can be extracted from LiDAR, including DEM and digital surface model (DSM), from which several data layers can be derived, e.g. slope, aspect, and hill shade. Different attributes of LiDAR data is used based on the study purpose. For the purpose of this study, height and intensity of LiDAR points are used (detailed discussion about the extraction method can be found in Section 4.1).

3.2.2 Raster data

Raster data provide a digital representation of real word in form of grids or squares. Available raster datasets are a DEM, from which several layers were derived (see Section 4.2), and a DDM. The DEM provides the elevation above the sea level of every pixel representing the main land or the islands

in the archipelago. On the other hand, the DDM provide a representation of the seabed with information on the depth of each pixel of it. The spatial resolution of the available DEM is 25 x 25 m, while for the DDM is 100 x 100 m. The DEM and DDM were merged into one raster layer where the shoreline (sea level) is assigned a value of zero, and higher (representing the land) and lower (representing the seabed) elevations and assigned positive and negative values, respectively. Figure 3.4 illustrates the study area combined from DEM and DDM.

3.2.3 Vector data

Vector data type is used in GIS to describe geometry and represent objects in the form of points, lines, or polygons [Harris et al., 2005]. Vector datasets available include the coverage of *Phragmites* along the Finnish coast of the Gulf of Finland, as well as fetch data along the shorelines in this area. The common reed coverage data is provided by University of Turku. The reed coverage file illustrates common reed growing coverage in the southern Finnish coast. This reed shapefile is generated from *Landsat* satellite images, it describes the common reed growing situation in 2001. Common reed growing areas are represented as polygons in different shapes and sizes. Figure 3.7 illustrated part of the common reed coverage.

The other vector dataset is the fetch given for along the shorelines of the mainland and islands in the study area [Ekebom et al., 2003]. Fetch is defined as the distance from a studied point to the nearest shoreline in a given direction ([Ekebom et al., 2003], [Hakansson, 1981] and [Tolvanen and Suominen, 2005]). It is used to indicate the openness of different segments of the shoreline (see Figure 3.6), an important factor which influences the processes and biota in the coastal areas [Ekebom et al., 2003].
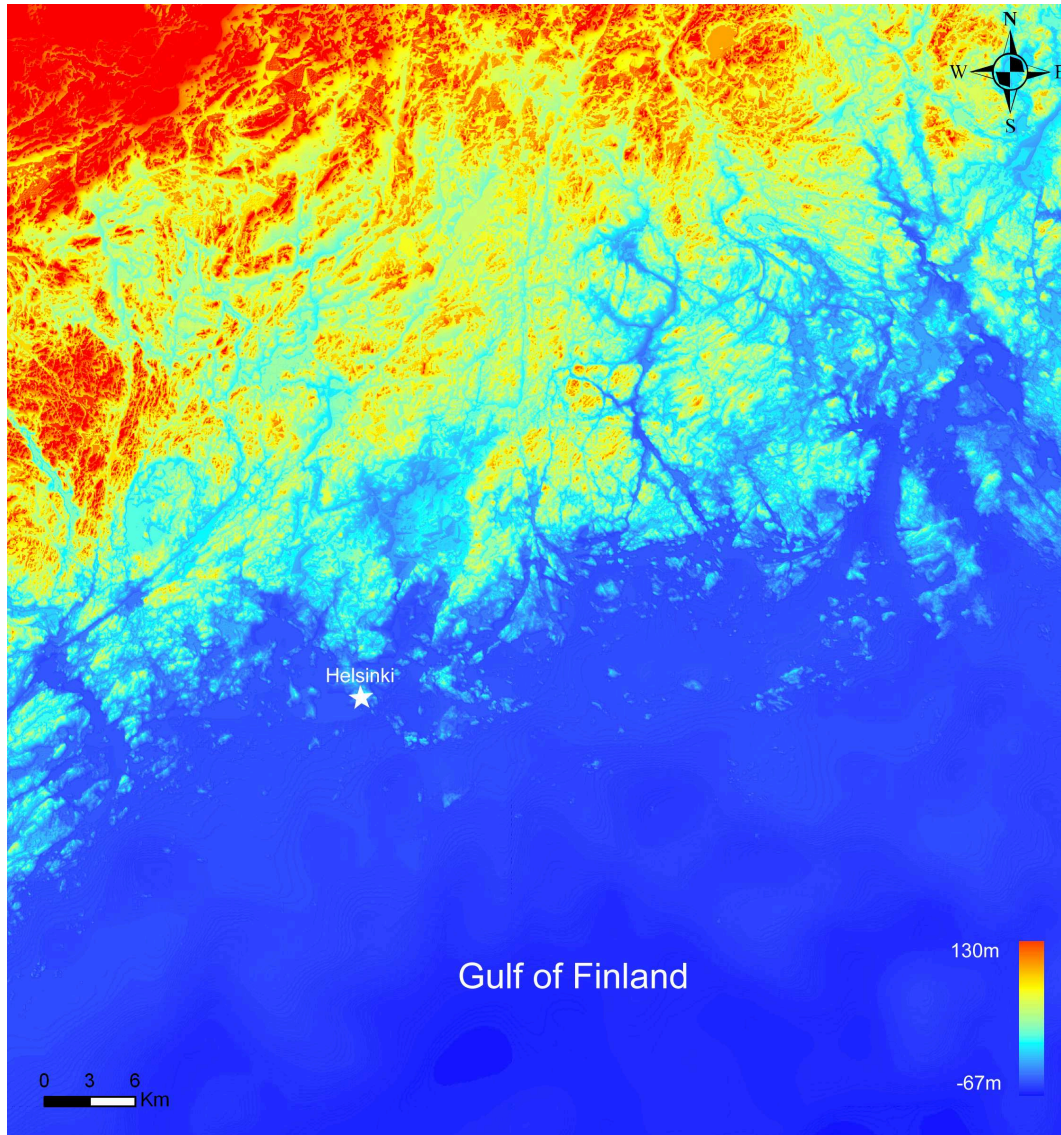
Figure 3.4: Merged DEM and DDM
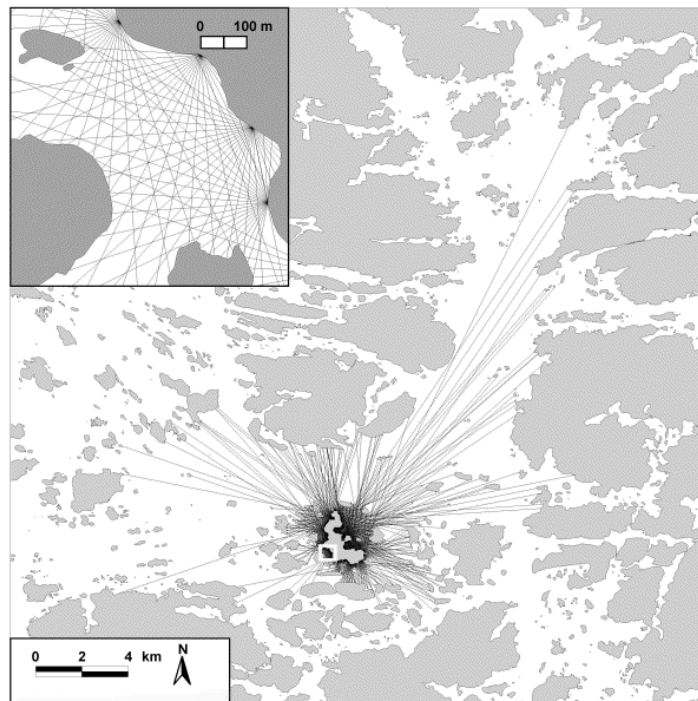
Figure 3.5: An example of the fetch data. *Source*: Ekebom [2003]
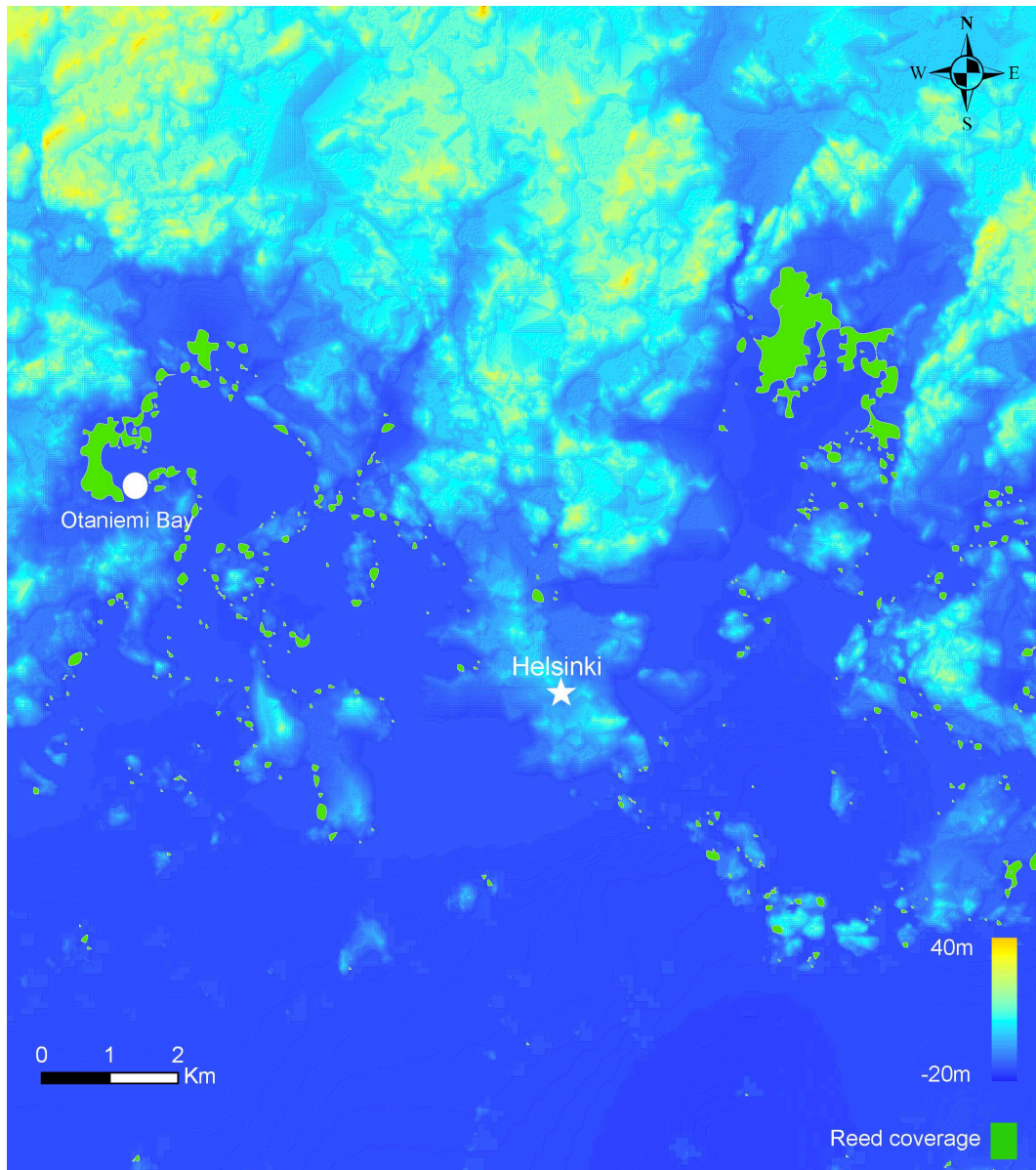
Figure 3.6: A sample of the common reed coverage

Chapter 4

Data Processing

In this chapter, the processing procedure of different datasets is described. Raw datasets, described in Chapter 3, had to be processed in order to provide the needed input for the developed model. Different types of data need different processing methods. The following sections describe the method by which reed coverage is delineated from the LiDAR data, methods used to prepare and derive needed layers from available raster as well as vector datasets.

4.1 Mapping of the common reed coverage

The main objective of LiDAR data processing is to delineate the common reed coverage in the corresponding area. Height and intensity, which are indicating the common reed, have been measured in a predefined reed growing area near Otaniemi. Since plant height and intensity remain similar in the same season, these two attributes can be applied entirely across the study area for the purpose of common reed coverage delineation.

4.1.1 LiDAR attribute analysis

As a laser altimeter, LiDAR measures the data range from a platform with a position and altitude determined from GPS and an inertial measurement unit [Koetz et al., 2008]. This inertial measurement unit determines final LiDAR data resolution. Essentially, they utilize a scanning device which defines the distance from the sensor to the ground, of a series of points approximately perpendicular to the direction of flight. If a laser pulse or a part of the pulse is

reflected from a roof top or the top of a canopy tree, the sensor will record the first return. Meanwhile, part of the pulse might partially penetrate the tree canopy and travel through it, to reach the ground. In this case, the sensor will record the return from the ground, i.e. the last return [Dickie, 2001; Webster et al., 2006]. By removing the first or last returns, a digital terrain model of ground surface topography or terrain can be generated respectively. Figure 4.1 illustrates the LiDAR cloud in study site.

Figure 4.1: LiDAR cloud in the study area

Besides height value, LiDAR data contains information of reflectance intensity of the surface (see Figure 4.2). The LiDAR intensity value refers to the corresponding spectral wavelength from the laser emits [Brennan and Webster, 2006; Webster et al., 2006]. Reflectance varies from material characteristics, as well as the light used; different materials have different reflectance. Consequently, intensity value provides useful information for the land-cover classification. Nevertheless, LiDAR intensity images often appear to be heterogeneous and contain data noise due to the excessive effect and artifacts caused by the sensor scanning [Antonarakis et al., 2008]. There are several methods for filtering LiDAR data noise, and here we introduce a technique for dealing with laser scanning angle. By filtering particular scanning an-

Figure 4.2: Representation of LiDAR intensity

gle of existing LiDAR data, and given certain height and intensity values, different classifications can be obtained from LiDAR data source.

Characteristics influence LiDAR data classification in several perspectives: elevation values determine the plants height, for instance *Phragmites australis* acquires dissimilar height attribute from bushes and trees; slope and aspect determine the tidal regime and wave exposure, which in turn influence the occurrence of intertidal species according to their specific ecological preferences, most likely the *Phragmites australis* grows in a flat sea area without large vibration [Hayball and Pearce, 2004]; and relative position of the sun and the sensor as well as the slope and aspect of the surface may produce responses according to topographic effect [Ikonen and Hagelberg, 2007].

4.1.2 Classification process

The accuracy of LiDAR classification depends on the ability to detect differences in vegetations height, which in turn depended on adequate height separation among community types [Bork and Su, 2007]. Across the study

area, dominance of height begins with sea level (0 meter), and progresses through reed plant area. Vertical height division lines between the higher vegetations such as common reed, bush and artificial forest are determined based on measurements of average height ranges.
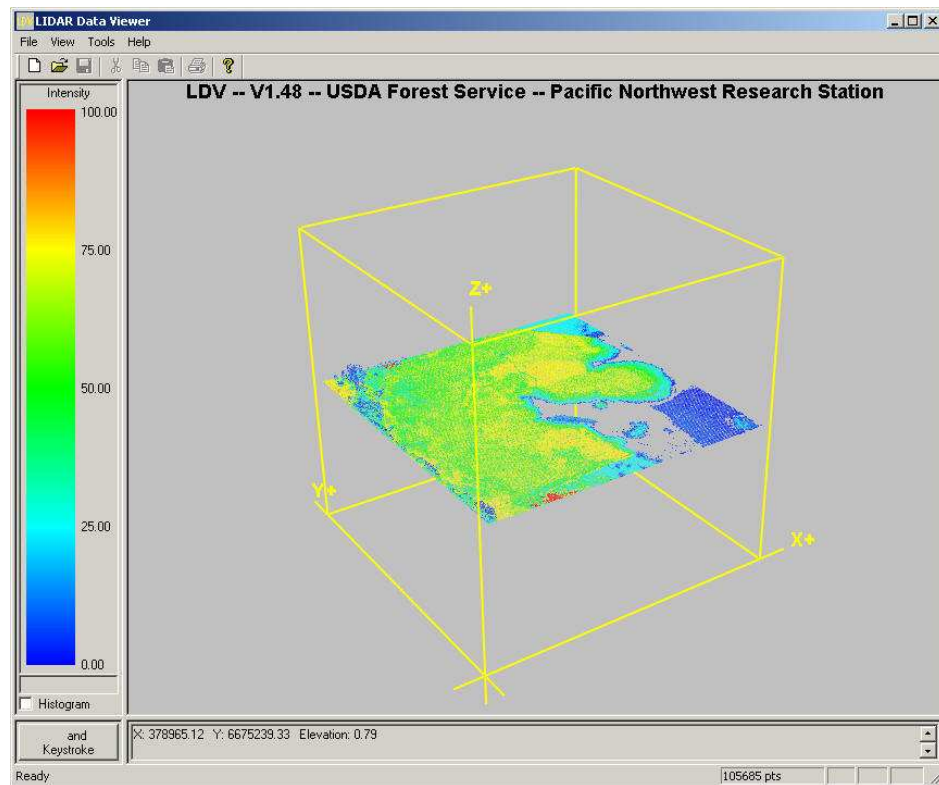
Figure 4.3: Analysis area

The LiDAR classification process requires accurate common reed attribute values. FUSION/LDV visualization system, an analysis software for measurement purpose, is used. The FUSION/LDV visualization system consists of two main programs, FUSION and LDV (LiDAR data viewer); while FUSION provides a typical 2D GIS interface allows users to select data, LDV contains the spatial-explicit data examination functions [Mcgaughey and Reutebuch, 2009]. With proper selection from the LiDAR cloud, the LiDAR height attribute can be measured in LDV (see Figure 4.3 and 4.4).

Measurement on selected sites indicates height value between 20 and 190 cm. This range is therefore considered as a criterion for common reed classification among vegetation.
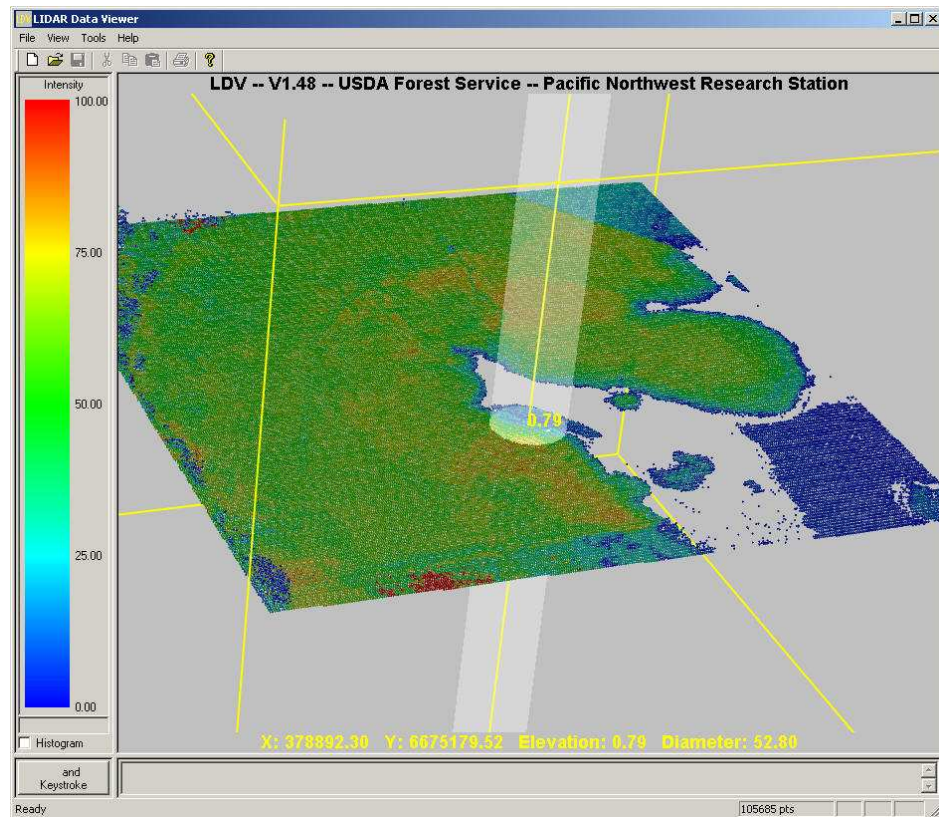
Figure 4.4: Measurement of common reed height in LiDAR cloud

Elevation begins with plain sea level at 0 meter; the class above sea level is sea waves. The *Phragmites australis* coverage above the sea level and waves is classified from the study area by differentiating between LiDAR data first and interpolated last return in the value of elevation. Discreet LiDAR data samples indicate that LiDAR points with a height less than 1.9 meters defines the upper boundary of the *Phragmites australis* class (see Figure 4.5). Meanwhile, the proportion of LiDAR points above 0.4 meter was the lower boundary determination for *Phragmites*. As a result, those range values are used as a division to separate open sea area and common reed coverage.

Intensity value of *Phragmites australis* from LiDAR data can be used as well to separate common reed area from the other classes similar in height to the reed. Figure 4.5 illustrates the image of intensity measurement in common reed area.

Wetland plants area distributes along the sea coast, their intensity value
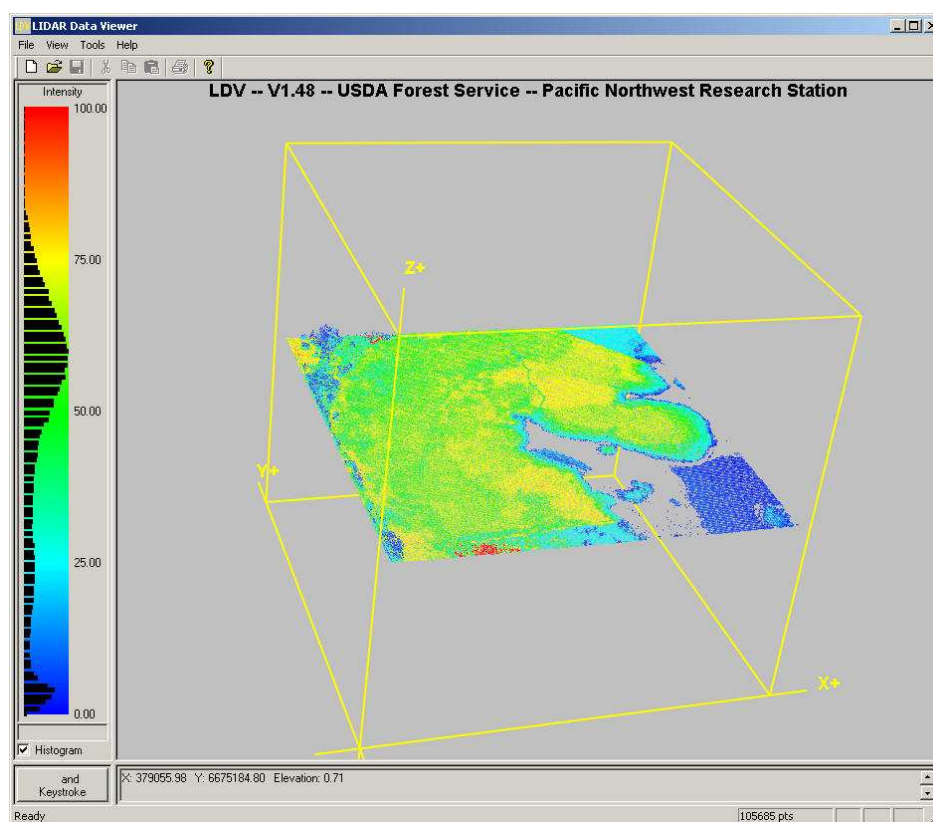
Figure 4.5: Intensity measurement of common reed in LiDAR cloud

various in a large range. *Phragmites australis* intensity has its own attributes, which drops in a certain range from 30 to 80 intensity values (see Figure 4.5). This measurement is performed under the LiDAR image intensity ranging from 0 to 255 in RGB. As a result, LiDAR derived intensity range information together with assistance of plant height can be used to distinguish *Phragmites australis* from other wetland features.

Phragmites australis in the study field is spread over plain sea surface with the slope vale less than 1°. The distribution is determined using LiDAR-derived DSM(Digital Surface Model). Slope gradient is calculated through surface analysis with a fixed pixel size, for instance 9x9 cell pixel radiuses. Cells are classified as being flat (less than 1°), gentle slope (1°to 3°), or steep (large than 3°). Aspect is classified into another system: treated as 0°from the sharp east direction, given clockwise rotation, it returns to east again with value of 360°. Aspect is then classified into 9 classes, including flat class which has the value of -1. From center on East clockwise to South-east, South,

Soeuth-west, West, Northwest, North, and north-east, with an incremental of 45°. As a consequence of its natural characteristic, *Phragmites australis* has a preference of sunshine facing trend [Gucker, 2010]. The collective aspect of South-east, South and South-west then are reclassified as slopes facing South.

Determinations for common reed flat area are above or below certain range of slope. *Phragmites australis* slope attribute near the land various in a larger range. The species in wetland also have different attributes compared with *Phragmites* field on the sea. However, in this research, wetland and inland area are beyond the range of analysis. Accordingly, common reed aspect preference became less important as an indicator of plant growing. As a result, this research simply utilities the slope and aspect values, approximately in full range, to classify *Phragmites* on sea surface.

With a combination of height, intensity, slope and aspect values, *Phragmites australis* can be extracted from LiDAR cloud as an invalidated classification. Figure 4.6 illustrates the classification flow chart.

Phragmites classification from LiDAR is validated against satellite images (provided by Google server). Accuracy assessment can be conducted by overlapping classified reed area with satellites images (see Figure 4.7). However, the validation process and accuracy assessment are not included in this research.
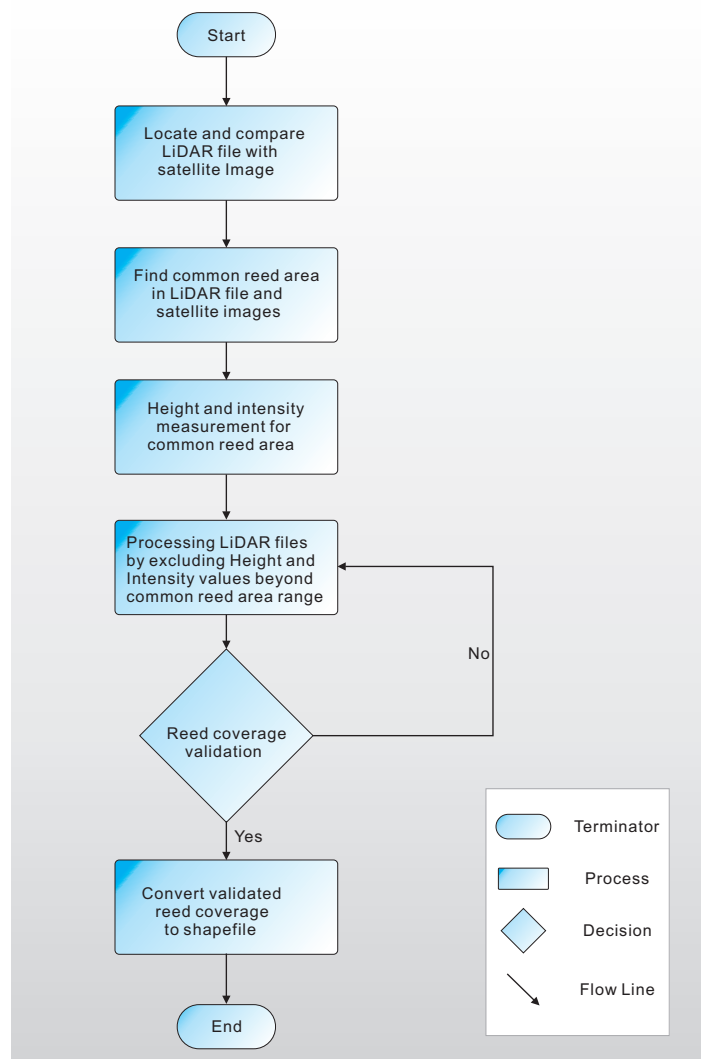
Figure 4.6: LiDAR classification flow chart
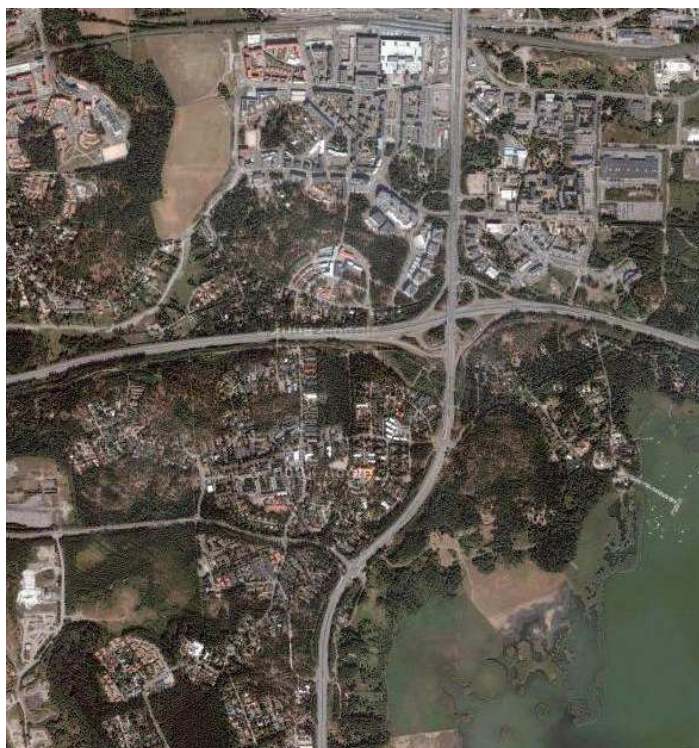
Figure 4.7: Satellite image in study area

4.2 DEM processing

Several topology attributes can be generated from the Digital Elevation Model (DEM) data, for instance slope, aspect, accumulation and stream network. In this research, open source applications and libraries are used in data processing. For instance, GRASS (Geographic Resources Analysis Support System) and QGIS (Quantum GIS) are used for DEM processing, modeling, and visualization.

Slope and aspect can be generated by GRASS function *r.slope.aspect*. The algorithm used in this function calculated slope and aspect using 3x3 neighborhood cell radius. Figure 4.8 and Figure 4.9 illustrate sample DEM data as well as the corresponding slope displayed in GRASS.
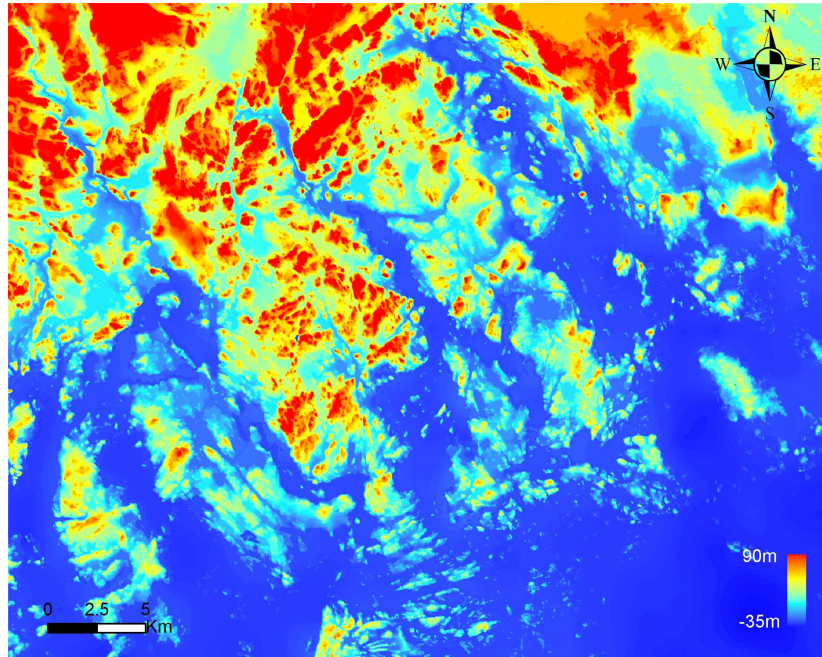
Figure 4.8: DEM
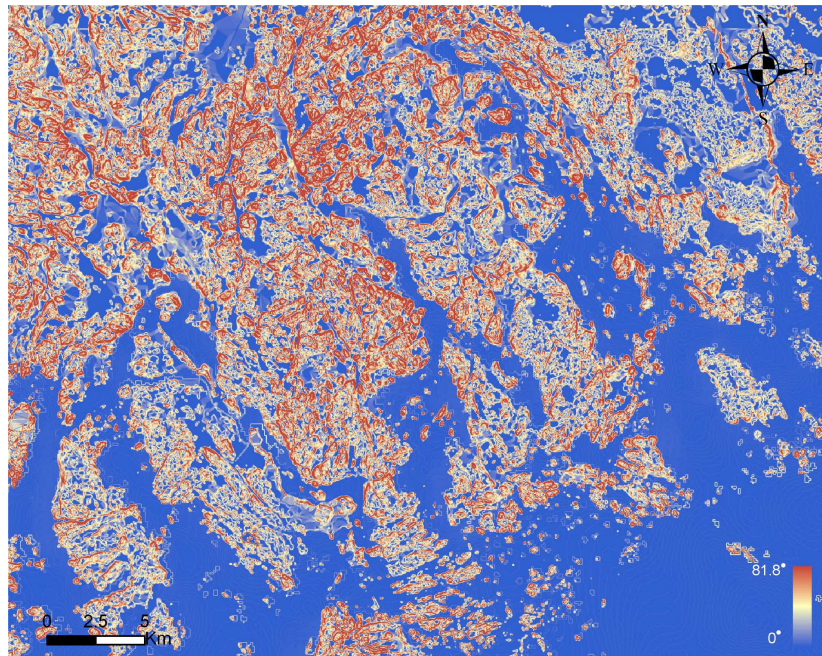
Figure 4.9: Slope derived from DEM

Accumulation is the pre-stage for stream network data analysis. Accumulation map can be generate by GRASS with *Hydrolic Modeling* module in raster processing. The module generates a set of maps indicating the location of watershed basins as well as accumulates value for pixels. With threshold describe the minimum size of an exterior watershed basin in cell, 4 map sets can be generated by this operation. The absolute accumulate value of each cell in the output map layer is the amount of overland flow that traverses the cell. This value is the number of upland cells plus one if no overland flow map is given. If the overland flow map is given, the value will be in overland flow units. Negative numbers indicate that those cells possibly have surface run-off from outside of the current geographic region. Thus, any cells with negative values cannot have their surface run-off and sedimentation, hereby considering the few amount of negative values, for simplification purpose negative number cells are excluded in this study.

Stream network or rivers have the ability of influencing common reed plant growing. River stream segments can bring nitrogen and other chemical influencing the common reed growing. With a proper input, stream segments can be extracting from the layer of accumulation by threshold values of each pixel. Small threshold values can generate a detailed stream network, and large values illustrate more generalized stream network. By given a suitable threshold value, river network can be extracted in GRASS.

4.3   Vector data processing

Processing methods of shapefiles include 2 major parts, methods for openness distance and open area calculation; the following 2 sections explain these methods respectively.

4.3.1   Distance computation

Waves are created by the friction between water and moving air over a certain length of open water surface [Harri Tolvanen, 2005], referred to as the fetch or openness vector data. For the openness data, each point has its own open distances. Given fetch lines were measured with a bearing of 7.5°areas around each point. The length of the radiating lines is chosen to be at least expected maximum distance. The openness distance lines are generated by cutting the lines parts not connected to the point at the shore. Therefore, open distances are the remaining lines length associated with the site centre

points on the shore over water to nearest land. Figure 3.6 illustrates the fetch lines in one site.

Several techniques are applied on the vector file of fetch lines to become usable by the analyses. The 48 lines around each point are abstracted into the regular 8 directions, namely N, S, E, W, NE, NW, SE, and SW. This research simplifies the openness distance data from 7.5°per sector to approximately 45°per sector. Original shapefile sectors start from 3.75°clock-wise direction, increase across 360°or 48 sectors, and then return to the original 3.75°the origin sector. The sectors degree positions are lack of 0°(North), 45°(Northeast), 90°(East), and etc. Therefore, the solution is using approximate degree position to represent the 8 directions. Table 4.1 describes the 8 directions and their corresponding sectors in degree. Table 4.1 N represent north, S represents south, E east and W west. Figure 4.10 illustrate the situation before selection (see Figure 4.10.A) and after selection (see Figure 4.10.B)

A. 48 sectors   B. 8 sectors
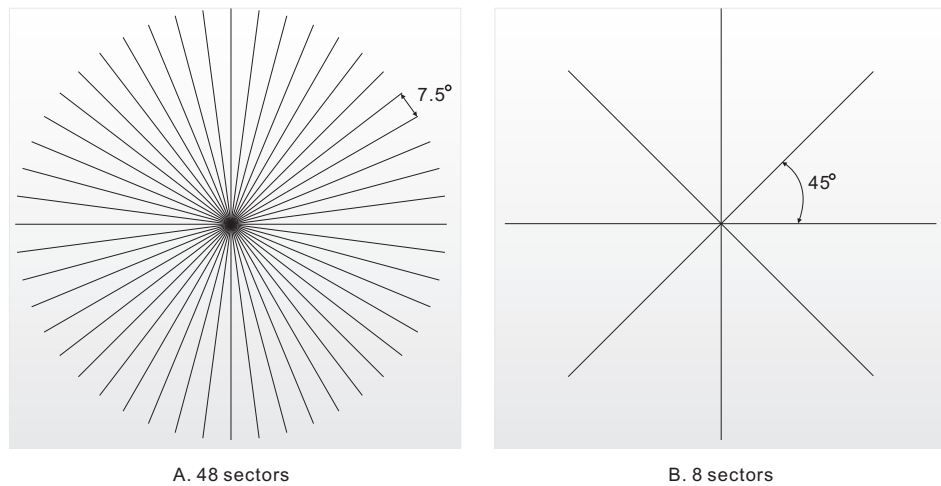
Figure 4.10: Sectors before and after selection

Degree	3.75°	48.75°	93.75°	138.75°	183.75°	228.75°	273.75°	318.75°
Direction	N	NE	E	SE	S	SW	W	NW

Table 4.1: Table for showing 8 directions and degree sectors

Simplification of vector data is the pre-stage of longest openness distance calculation. Amongst the 8 fetch lines around each point, the longest fetch is determined and its direction is assigned as the open side of the location. The openness direction calculation is done by the code shown in Listing

4.1. Openness directions assign more influence on the decision of the site open attribute, for instance points near river mouth are less open than site near islands. The openness attribute is employed to facilitate to analysis linkage of common reed coverage location and the corresponding site openness attribute. Table 4.2 describes the open distance calculation result.

```
1  Sub  OpenDistanceCal

3        Dim  A(8)  As  Double
         Dim  MaxEdge  As  Double
5        Dim  OpenDirection  As  Integer

7        A(1)  =  [FETCH_375]  :  A(2)  =  [FETCH_4875]  :
         A(3)  =  [FETCH_9375]  :  A(4)  =  [FETCH_1387]  :
9        A(5)  =  [FETCH_1837]  :  A(6)  =  [FETCH_2287]  :
         A(7)  =  [FETCH_2737]  :  A(8)  =  [FETCH_3187]

11
         For  i  =  1  To  8

13
                 If  A(i)  >  MaxEdge  Then
15               MaxEdge  =  A(i)
                 OpenDirection  =  i
17               End  If

19       Next

21  End  Sub
```

Listing 4.1: Open distance calculation

Direction	N	NE	E	SE	S	SW	W	NW	MaxDirection
	0	0	24	46	411	111	0	0	South
Distance(m)	0	18	80	1428	591	0	0	0	Southeast
	0	0	181	87	590	3499	0	0	Southwest

Table 4.2: Example result for openness longest distance

Chapter 5

The Simulation Model

This chapter presents the methodology study of this research, which can be expressed as common reed growing condition and cellular automata expansion modeling. These 2 separate theory parts are merged into expansion model, which is used for simulating common reed growing in the Gulf of Finland. This chapter explains the principles in section of model structure and the following application implementation section describes the practical simulation model program.

5.1   Model structure

Cellular automata models are dynamic and discrete in time, space and state. Simple cellular automata is defined by function (f), states (S), and neighbors (N). Three factors have the relationship in Equation 5.1:

$$S_{t+1} = f(S_t, N) \tag{5.1}$$

In the above equation, S defines the finite set, f is transition rule function, t refers to transition discrete time or generation and N is the cell neighborhoods of current generation.

According to Wolfram [1984], standard cellular automata contains of a set of identical cells, and discrete cell states, cell neighborhood function, transition rules and discrete time steps which refers to generations or year. One cell should be in set of possible states, update in accordance with the interaction rule. The update progress should be non-deterministic or stochastic, since the nature phenomenon contains proper degree of uncertainty.

5.1.1   Universal environment

A discrete two-dimensional universe is adopted in this study as the main goal is determining the expansion of the reed coverage in the archipelago represented in a 2D manner. The two-dimensional universe is a gridded surface, similar to chessboard (Figure 5.1). This representation is also similar to the raster data format in GIS in which some datasets are given, e.g. digital elevation model (DEM). The CA model gains great benefit for data processing because of the similarities between grid and raster structure. The CA approach allows fast and accurate simulations of repeated predefined rules based on digital elevation models (DEM) [R.Minkoff et al., 1992] and other raster data layers which provide information related to theecological processes in question [Fonstad, 2006].
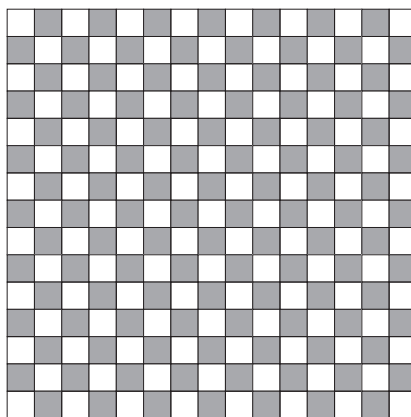
Figure 5.1: Adopted 2D CA universal environment

Space of CA universe

As a method for storing and displaying spatial data, raster format is divided into rows and columns, which form a regular grid structure (see Figure 5.2). Although cells of raster do not necessarily have to be squares, in the present CA model, square cells are used to comply with the existing datasets. Each cell within a matrix or grid in Figure 5.2 contains location coordinates as well as an attribute value. On the other hand, each raster layer represents a factor related to process of reed expansion, including elevation, slope, nutrients, and land use. The top raster layer represents the coverage of *Phragmites*. For each layer, different color represents the cell values, for instance, elevation layer have higer value in red cell and low value in blue cells; reed coverage

green color represents the reed existing area, and blue is the potential area
that reed can expand (Figure 5.2).
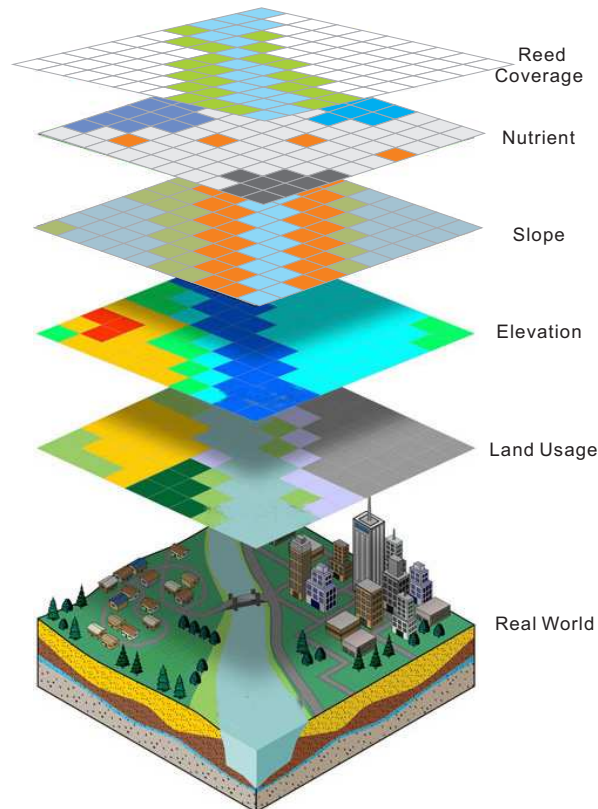
Figure 5.2: Representation of the real world in raster format

The spatial resolution in raster representation is controlled by the cell (pixel).
A single cell represents an area covered on the ground, and higher spatial
resolution indicates more pixels per unit area. A cell size of 1x1 m was
chosen to represent the layer of reed coverage and other factors. The cell
size chosen was relatively small in order to comply with the nature of the
phenomenon being analyzed, namely the reed expansion. In order to make
all layers compatible for the calculations within the model, raster layers with
different cell sizes were resampled into a spatial resolution of 1x1 m. An
example of the resampled layers is the DEM; available DEM was originally
of 25x25-m-cell meaning that a single cell covers an area of 625 m^2 on the
ground, an area much larger than how much reed can propagate in one time
step (a year). Illustration of the cell size in relation to the spatial resolution
is provided in Figure 5.3. The effect of resolution on the raster representation

is illustrated in Figure 5.4.

16x16 cell size 1m   8x8 cell size 2m   4x4 cell size 4m
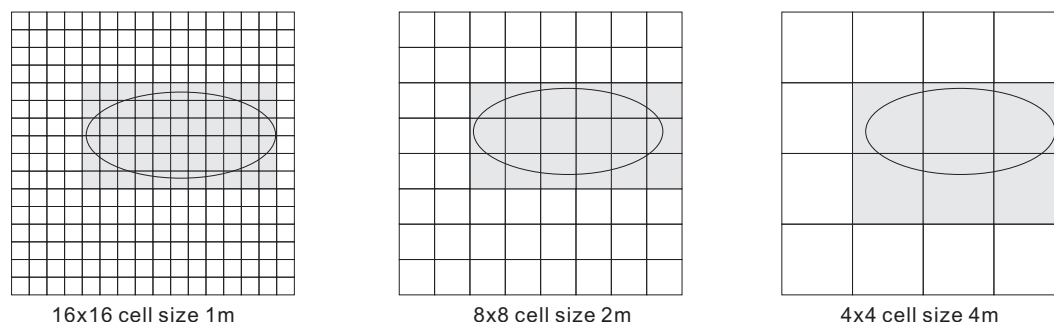
Figure 5.3: Representation of the space in different cell sizes

Cell size 15m   Cell size 15cm
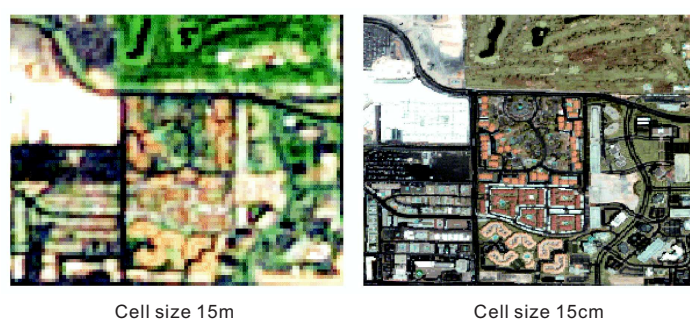
Figure 5.4: Cell size effect on the spatial resolution

Time in CA universe

Time is another essential element in the CA model. Discrete time in the CA model indirectly reflects the actual time. In that sense, there are two possibilities: expansion is faster than real situation, or slower. Therefore, in order to build a realistic simulation model, expansion speed in the CA model needs to be calibrated properly. Instead of chaning the raster map resolution, several methods can be used concerning CA time. The CA model contains grid cell is 25x25 meters; CA principle constrains the condition of growing at the speed of 1 cell at 1 discrete time step (equals to 1 generation). During this process, common reed spreading speed is 25 m per 1 discrete time step, assume 1 generation reflects to 1 actual year time, and then the speed would be 25 meters per 1 year. Obviously, the plant spreading speed is

over estimated, therefore time needs to be calibrated to slow down common reed spreading speed.

Various methods can be used in simulation calibration and each method cause different consequences. Consider CA model simulation is slower than real-time, in this case, no calibration need to be set in CA model. Since the CA model gives slower simulation, then CA model can be treated in a different way. For instance, the previous assumption of one CA model is 1 generation per 1 year, if CA simulation is slower than expectation, previous assumption can be changed into a smaller scale. Suppose the CA simulation is 4 times slower than real-time situation, then the solution is adjust CA time assumption to 0.25 year. Accrodingly, 4 generations need to be operated in order to simulate 1 year reed expansion.

In case CA model expresses simulation faster compared with real situation, the solution can be described as follow. CA model have the origin attributes "NotGorow" or "Grow" minimum 1 cell per discrete time step. Figure 5.5.a illustrates the normal CA simulation, from time "T=0", "T=1" and "T=2" the plant is "NotGrow". The cell starts to expands suddenly in the 3th generation "T=3". However, this case does not match the real plant growing situation. In reality, plant grows or shrinks gradually at an average speed in 1 year. To solve this problem, this research introduces a method used in current CA model called "probability accumulation". Instead of assign cell probability value 0 (not grow) or 1(grow), a value in defining range [0, 1] is calculated and assigned to each cell (see Figure 5.5.b). "Probability accumulation" gives the possibility to cells to grow from 0 to 1 in several steps compared with previous 1 step. In Figure 5.5.b, the cell expands averagely, which gives the possibility for plant to occupy "half cell" per generation. Thus, Figure 5.5.b with "probability accumulation" method simulates a closer scenario compared with Figure 5.5.a. While the probability accumulate, the cell becomes more suitable for common reed growing, and consequently have the value of reed occupation accrodingly.

5.1.2   Cell neighborhoods

Frequently used neighborhood templates for 2-dimensional square grids are Moore-neighborhood consisting of central cell and eight adjacent cells, and von Neumann-neighborhood, which contains the central cell and four adjacent cells. The corresponding transition rules can be deterministic or stochastic; it can be described in following Equation 5.2:
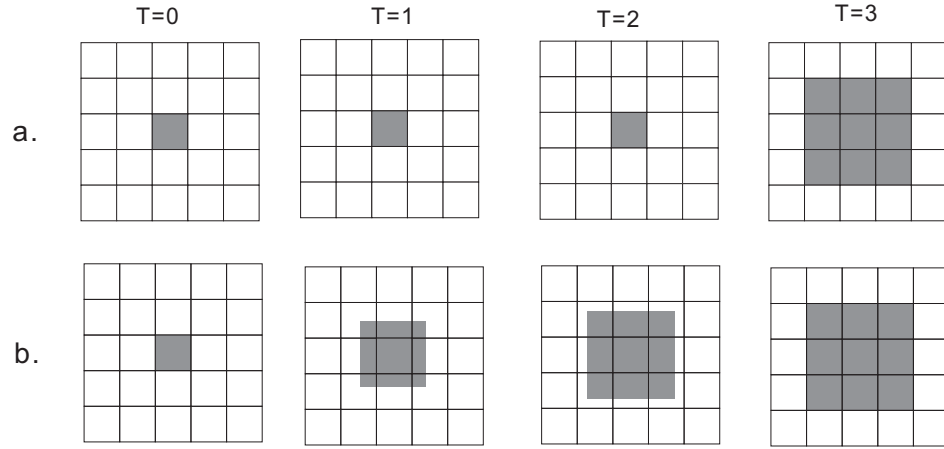
Figure 5.5: Two methods in calculating growth probability

$$A_{t+1}^s = f(A_t^{s-r}, A_t^{s-r+1}, ..., A_t^s, ..., A_t^{s+r-1}, A_t^{s+r}) \tag{5.2}$$

A_t^s in Equation 5.2 represents the cell s at generation t, r is the radius of cell neighborhoods, function f represents the transition rules. In Conway's life [Gardner, 1970], A_t^s also refers to the cellular automata configurations at discrete time step t.

5.1.3 Cell status

Cell status in normal cellular automata are simple. For instance, in Conway's Game of Life [Gardner, 1970], cell status are integers set as 0, 1, 2 and etc. Those cell status make the computation simple and effective. Nowadays, as computer becomes powerful, it allows floating point cell status values to be calculated efficiently. Since floating numbers are not infinite, cell status defined by floating numbers is still discrete.

In the prototype of common reed spreading CA model sets, cell states are integers. Value 0 denotes that reed does not exist, and value 1 denotes that reed exists or the cell satisfies plant spreading conditions (in the future generations). The disadvantage of the integer cell status in CA model contains the disadvantages is that it constrains the cell spreading by a minimum of 1 cell per generation. This means that the common reed expands by 25 meters in 1 discrete time step, which is overestimated.

Primary status

The aforementioned "probability accumulation" method involves float point instead of integer values while calculating cell status. Cell value represents the probability of common reed existence, ranging from given domain [0, 1]. In this domain, cell have a infinite number of status, which ranges between 0 to 1 and including value 0 , 1 themselves. Assume the initial value of one cell is 0, it has the possibility to grow reed plant in unknown future generations. This means the cell value change from 0 to 1 in several discrete time steps, meanwhile cells with the value 1 change to 0 also can take more than 1 discrete time step.

Four hypotheses can be made from the cell states changing procedure: *a.* cell value 0 become cell value 1; *b.* cell value 0 stay unchanged; *c.* cell value 1 becomes cell value 0; *d.* cell value 1 status stay unchanged. Figure 5.6 illustrates these four hypotheses, Figure 5.6 also gives an example for selected cell changes from 0 to 1 and 0 to 0.
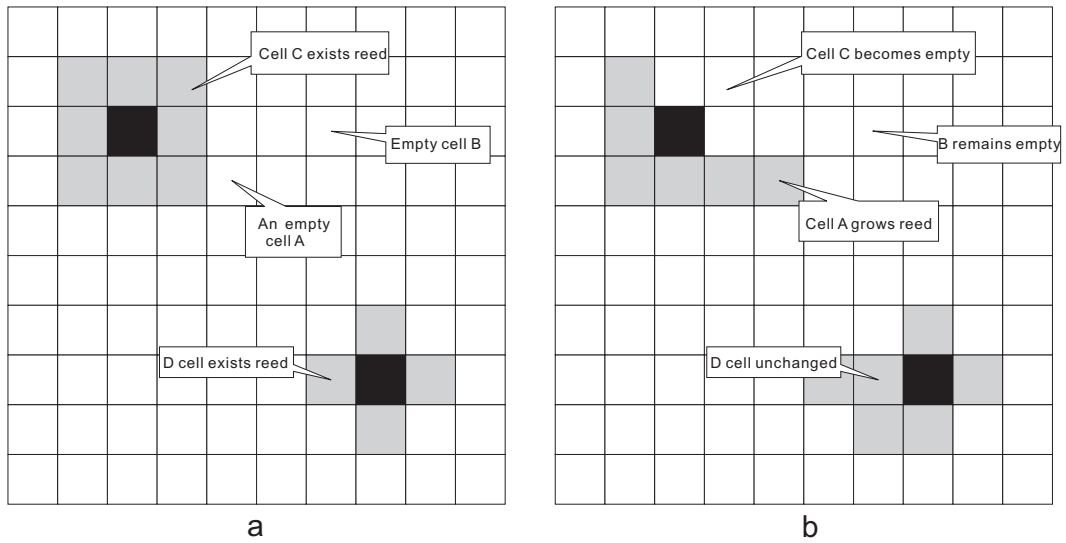
Figure 5.6: Change in cell status

Status threshold

The criteria to decide whether common reed growing , not growing, or dying is the cell value. Simple method of calculating the growing and dying status is set cell value of 0 to "NotGrow" and set cell value of 1 to "Grow", but this might encounter problems. Take a growing cell with initial value 0 for example, this cell will become occupied by common reed in several discrete time steps, thus its cell value need to become 1 at the final stage. However, the calculation functions in our CA model give a float number less than 1 instead of integer 1. To solve this problem, a threshold need to be set in CA model (see Figure 5.7), if the calculated value is larger or equal to this threshold the cell will become occupied by reed, otherwise the cell is partially occupied by common reed. Instead of possibility distributes averagely in [0, 1], the threshold allows the final layer to have only 2 values "0" and "1". Meanwhile, the other threshold is set for common reed exist to absent, the corresponding cell value changes from 1 to the threshold. During this process, if the cell value becomes smaller than threshold the cell become absent for common reed, if larger or equals to the threshold cell is partially occupied by reed plant and the cell value represents reed density in cell itself.

By involving status threshold, previous cell status processing can be completed in a different mean. Cell value calculated by transitional function mostly drops between the define range (0, 1). Such a low percentage "Not-
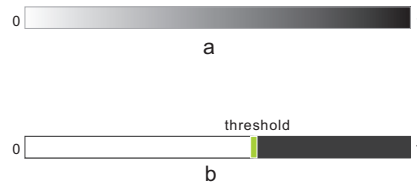
Figure 5.7: Threshold decides cell status

Grow" and "Grow" cell cannot satisfy currently CA simulation model in the actual situation for common reed spreading. Unlike previous explicit cell status where 0 represents "NotGrow" and 1 represents "Grow", threshold can be set to proper value in CA simulation. Threshold value has an impact on common reed spreading speed, take the maximum threshold as an example, the closer it is set to value 1 the slower spreading speed will be; the closer it is set to value 0 the faster spreading speed will be. Therefore, threshold can be adjusted to a proper value to give an optimal spreading speed. Proper threshold in CA simulation has key impact on the degree by which the CA model matches the actual situation of common reed growing.

5.1.4 Transitional rules

Transitional rules meet the top-down [1]approach characteristics, by breaking down a system to gain insight into its compositional influential factors. An overview of CA model is first formulated, which gives the phenomenon of common reed spreading. Then the influential factors (nature phenomenon) refine more details, sometimes factor contains sub-level elements. The CA model is not complete until the entire specific influential factors are divided into basic elements. With each element is corresponding to 1 transitional rule, the CA model is formulated by compiling transitional rule elements.

Influential factors related to the common reed expansion vary in large categories. Factors can be divided into different perspectives; they are year-independent, year-dependent and the influential neighborhoods factors. Yearly independent implies that factors are not affected by the year changing; for instance elevation and slope remain unchanged from time to time. Year dependent factors include ice condition, winter temperature, ocean currents, etc. Besides the two types of influential factors, neighborhood condition, which directly linked to the surrounding common reed growing situation, is

---

[1]The conceptual understanding of environmental dynamics can be described as top-down process.

another important factor in common reed expansion.

$$P_{ij} = f(W_1 \times F_1, W_2 \times F_2, W_3 \times F_3, ..., W_n \times F_n) \tag{5.3}$$

The developed cellular automata model is probabilistic; the transition rules calculate the values for representing status change. The value of each cell corresponds to the possibility of growing common reed. The Equation 5.3 above illustrates the transition calculation function for common reed existence possibility. P_{ij} refers to the probability value for certain cell in the grid to be reed-occupied, and in P_{ij} i and j is cell location in defined the coordinates system. Current raster CA model use grid and ij represents for column and row respectively. f is the calculation function or combined functions; to find proper transition formular, CA model needs to be run several times and *Model Validation* (see Figure 5.9) can be also used to define suitable transition calculation formulae. Moreover, *Model Validation* requires successive multi-temporal common reed coverage data, in order to compare the CA simulation results and actual reed coverage data, so that the accuracy can be assessed.

F_n in Equation 5.3 represents factors, which affect the common reed growing. Hereby, the factors can be divided into the following types: spatial factors, ecological factors, human factors and neighborhood states. In order to calculate factors in transition functions, factors need to be broken down into elements: elements present spatial factors including elevation, slope, hill-shade; ecological factors including salinity, nutrient level, as well as the other plant species, animals, micro-organisms; human factors include work related to construction, seashore conservation, pollution and other activities that affect reed spreading.

Factors contain different influential importance for common reed spreading in CA model. Therefore, the importance of each factors have to be directly reflected in transition functions, which is why weight W_n is assigned to each factor. Assume the number of influential factors is n, and each factor has different weight in determining the probability. Since factors affect common reed growing are excessive, instead of including all actual factors inside CA model, potential factors are chosen in transition formula. Potential factors have adequate weights to influence the final probability.

5.1.5   Edge effect

Instead of no-boundary condition, CA models usually contains solutions for boundaries. An simple method to avoid the edge effects of boundary is to make CA models universal environment large than the given area, and assign those extra pixel a suitable single value [Janssens, 2009]. But this increases the use of computing resource. Solution in the common reed expansion case is different, by generate an rule using IF-THEN in transition, the border cells rules can be different. For instance, in Figure 5.8 A, the corner pixel has 3 neighbors instead of 8, mid-edge pixel in Figure 5.8 B contains 5 neighbors other then its original Moore neighborhood.

A) Corner cells   B) Mid-edge cells
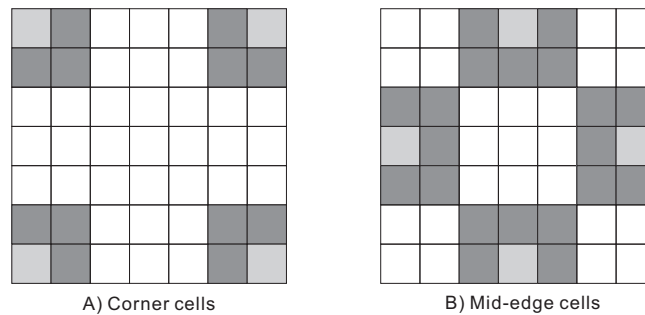
Figure 5.8: Edge effect solution

5.1.6   Monte Carlo method in cellular automata

Monte Carlo methods are useful for modeling phenomena with uncertainty inputs, which is the case the common reed expansion. Common reed expansion situation contains significant uncertainty. It is infeasible or impossible to compute an exact result with a deterministic algorithm for *Phragmites australis* expansion. *Phragmites australis* is able to avoid physical and biological stresses by a accessing distant resources and ameliorating local conditions, [Burdick and Konisky, 2003]. This devotes *Phragmites australis* characteristic of sharing materials over distances measured in meters rather than decimeters. Consequently, this also creates uncertainty in common reed expansion process.

Besides the aforementioned characteristic, other factors bring uncertainty to common reed expansion as well. Elevation or water depth has a major influence on *Phragmites australis* expansion. The water depth various in

different time in certain coastal land area influenced by tidewater. The phenomenon cause abnormal distribution of common reed, some plant might grow in deep water while there is no common reed spring up in shallow area. Moreover, the other influential factors include area, slope, winter ice area, human construction along the coast, and almost most of the other factors contribute to the uncertainty in CA simulation model.

Implementation with Monte Carlo method in CA is represented mainly in the transition rules. The decision of becoming occupied by common reed or not is effected by uncertainty, therefore in the process of making decision in CA generation, of each time step, the model require random number. For instance, one subversion transition rule can be written as *IF* the current calculated cell probability dropped in the range of 0.6 to 0.7 , *THEN* cell have 75% chance to become occupied by common reed in next discrete time step. This transition rule requires random number between 0.6 to 0.7, additionally the chance of becoming common reed should be set as 75% with randomness. This can be achieved by setting a predefined random number range from (0,1) and assign the random number to be true with condition less than 0.75. As a consequence of the randomness, the CA model needs to be run several times, then finalized with a probability distribution model.

5.2 Cellular automata process diagram

The previous section described all elements utilized by cellular automata simulation process. The entire cellular automata simulation model is illustrated as a flow diagram in Figure 5.9. It starts with the *Initial Reed Coverage*, which refers to the current common reed coverage, which configures the state for each cell (S_t) model at the discrete time t. Then, in the following step (namely, *Compute Possible Transition Probability Vectors*), the possibility of cell S_t to become occupied by the common reed is calculated. This calculation consists of 2 components, *Cell Suitability* and *Neighborhood State*. Cell suitability decides how suitable the location is for reed, while neighborhood state verifies the cell neighborhood condition. Those 2 components contribute to the calculation of the probability of a cell to be occupied by the common reed.

The process proceeds to *Monte Carlo Selection for* S_{t+1}, which is described in Section 5.1.6. Then, S_{t+1} represents the cell state in discrete time step $t+1$, which is the predicted state of the cell in question in the next generation. The resultant reed generation needs to be validated in order to evaluate the accuracy of CA model output. *Model Validation* can provide calibration for

CA model itself. In order to calibrate the parameters of transitional rules, the model needs to be run several times.
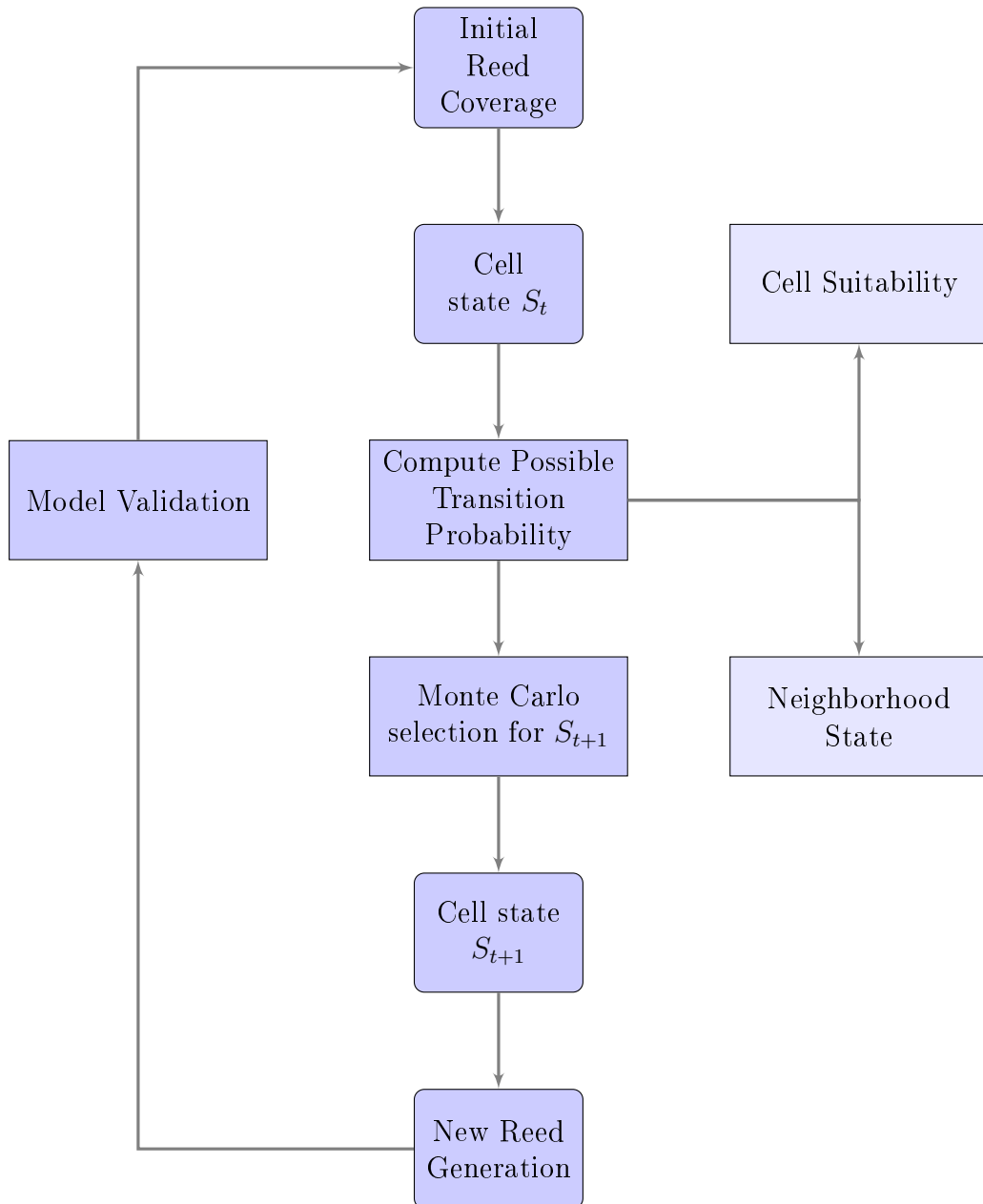
Figure 5.9: Flow diagram for the cellular automata model

5.3   Model implementation

The programming language used in this computational CA model is JAVA. The simulation is done in a raster 2D space. Several raster maps represent different conditions, such as common reed coverage, elevation, and slope. Based on the values in each cell, the probability of cell to become occupied by the common reed in the next discrete time step can be calculated according to the predefined rules. Each cell value is calculated during the iteration through the 2-dimensional space, and results are stored in an array defined according to the original raster maps.

5.3.1   Neighborhood algorithm

The algorithm in Listing 5.1 describes the neighborhood number counting for inner cells without boundaries. Algorithm is initialized by reading the common coverage layer, 2 functions are used to acquire total number of rows and columns separately. Then the algorithm assigns a 2-dimensional array $cellNeighbours$ with $cellCols$, $cellRows$ as column and row number. Iteration starts from $x = 1$, $y = 1$ and end at $x < cellCols - 1$, $y < cellRows - 1$, the loop iterates through all non-boundary cells. During the iterations if the cell fulfils the requirement of $reedLayer.getAttribute(x, y) > 0$, since common reed exist in this cell, and neighborhood number starts counting in 8 conditions.

```
1   /* general neighborhood number count without edge solution */

3       /*get total number of reed layer rows*/
        cellRows = reedLayer.getNumRows();
5
        /*get total number of reed layer column*/
7       cellCols = reedLayer.getNumCols();

9       /*create new array with accroding to raster row and column numbers*/
        cellNeighbours = new int[cellCols][cellRows];
11
        /*iteration through whole raster map*/
13          for (int x=1; x<cellCols-1;x++){
                for (int y=1; y<cellRows-1;y++){
15
        /*get attribute of the current cell decide whether reed exist or not*/
17                          if ( reedLayer.getAttribute(y, x) > 0   ) {

19      /*increase its neighbors cells Buffer with value 1 if condition is true*/
                                cellNeighbours[x-1][y-1]++;
21                              cellNeighbours[x][y-1]++;
                                cellNeighbours[x+1][y-1]++;
23                              cellNeighbours[x-1][y]++;
                                cellNeighbours[x+1][y]++;
25                              cellNeighbours[x-1][y+1]++;
                                cellNeighbours[x][y+1]++;
27                              cellNeighbours[x+1][y+1]++;

29                          } /*end if*/
                    }/*end for*/
31          }/*end for*/
```

Listing 5.1: Algorithm for general neighborhood withoutboundary cells

The algorithm in Listing 5.2 illustrates neighborhood counting for edge cells in raster grids. 8 different conditions represents 8 neighbors, each of them has influence on the cell neighborhoods' number. By changing incremental value dx and dy, the algorithm calculates the number of neighbors for the edge cells on the raster map. Since incremental values on x y directions are 1 and 0 respectively, and the calculation starts with cell in coordinate $(1, 0)$. Default incremental value dx equals to 1 and dy equals to 0, the calculation begins with the bottom edge cells. These tow value ensure the algorithm calculation through the bottom edge from left to right. Then right edge cells are preparaed, by applying similar principles, $dx = 0$, $dy = 1$ operates calculation through right edge cells. $dx = -1$, $dy = 0$ operates top edge cells, incremental values $dx = 0$, $dy = -1$ operates on left edge, the edge cells calculation finalize with $x = 0$, $y = 0$ in the coordinate origin.

```
1  /* neighborhood count algorithm with edge solution */

3  /* initialize with coordinates at (1,0), down edge counter-clockwise direction*/
        int x=1; int y=0;
5
   /* incremental on x direction with value 1 and y direction 0 */
7        int dx=1; int dy=0;

9  /* starting the iteration */
        while( true ) {
11
   /* if reed exist in current cell */
13       if ( cells[x][y] ) {

15           /* neighborhood edge in 8 different conditions, represent 8 neighbors*/
                if ( x > 0 ) {
17                   if ( y > 0 )
                     cellNeighbours[x-1][y-1]++;
19                   if ( y < cellRows-1 )
                     cellNeighbours[x-1][y+1]++;
21                   cellNeighbours[x-1][y]++;
                }
23               if ( x < cellCols-1 ) {
                     if ( y < cellRows-1 )
25                   cellNeighbours[x+1][y+1]++;
                     if ( y > 0 )
27                   cellNeighbours[x+1][y-1]++;
                     cellNeighbours[x+1][y]++;
29               }
                 if ( y > 0 )
31               cellNeighbours[x][y-1]++;
                 if ( y < cellRows-1 )
33               cellNeighbours[x][y+1]++;
                 }
35
       /*edge cells neighborhood*/
37
       /*incremental value through right edge*/
39           if ( x==cellCols-1 && y==0 ) {
                 dx = 0;
41               dy = 1;

43       /*incremental value on upper edge*/
             } else if ( x==cellCols-1 && y==cellRows-1 ) {
45               dx = -1;
                 dy = 0;
47
         /*dealing with left edge*/
49           } else if ( x==0 && y==cellRows-1 ) {
                 dx = 0;
51               dy = -1;

53       /* when iteration goes to original point (0,0) jump out loop */
             } else if ( x==0 && y==0 ) {
55
             /*default incremental value dx==1 dy==0 operates on down edge*/
57                       /*all edge cells done*/

59               break;
         }
61
   /*give new x and y value with corresponding incremental value dx and dy*/
63       x = x + dx;
         y = y + dy;
65
   }/*end while*/
```

Listing 5.2: Neighborhood solution for edge cells

5.3.2   Growth probability calculation

The calculation of growth probability can be divided into 2 parts (see code
in Listing 5.3). The algorithm starts with checking the status of factors.
The CA model in this model is constructed using Moore neighborhood with

neighbours. The neighbor cells have a large influence within CA model struc-
ture. The calculation starts with multiplying the number of neigbors value
with corresponding weight value. Factor weight is calculated according to
transition rules to ensure final probability ranges from 0 to 1 (see Equation
5.4), consequently the final probability can be obtained from factor prob-
ability and their weights. Weights are assigned to the explanatory factors
with respect to their influence on determining the suitability of a cell for
reed. Therefore, factors deemed strongly influential for the phenomenon are
assigned higher weights compared to those considered less important. P_{ij}
represents one cell in the raster map in row i, coloumn j. f is the functions
for calculating the probabilities. While F_n represents the explanatory factor,
W_n is the weight assigned to the explanatory factor.

$$P_{ij} = f(W_1 \times F_1, W_2 \times F_2, W_3 \times F_3, ..., W_n \times F_n) \qquad (5.4)$$

The following Listing (5.3) presents the algorithm for calculating growth
probability. It begins with reading data for factor layers and common reed
coverage, then calculating the probability of common reed expansion into
the cell in question. Afterwards, the algorithm applies the neighborhood
condition. A new raster layer is resulted which represent the predicted reed
coverage in the next year or discrete time step.

```
1
    /* common read factors and common reed cover data */
3   INITIALISE CA application (includes edge cells)

5   BEGIN CA simulation iteration

7       For each cell M
            M.slope = slope value of cell  M
9           M.elevation = elevation value of cell M
            M.factorX = value of factor X of cell M
11          .
            .
13          .
            IF cell M is edged cell
15              THEN M.neighbor = number of edge neighbors
            ELSE
17              M.neighbor = number of neighbors

19  /* calculate the probability of cell M */

21      P = W.slope * M.slope + W.elevation * M.elevation + W.factorX * M.factorX
            + ... + W.neighbor * M.neighbor
23  /* Produce new generation based on Probability value P*/

25  END of CA simulation iteration
```

Listing 5.3: Implementation of idealistic growth calculation function

However, the general probability calculation function requires sufficient data,
and proper weights assigned to each influential factor. Since currently avail-
able datasets are limited, an alternative probability calculation function is
constructed differently (the results shown and discussed in the following
Chapter are generated using the CA model based on this alternative func-

tion). For each cell within the grid, the elevation and slope are acquired and compared with the predefined common reed growing condition . The function is as follows: *IF* the elevation and slope are suitable for reed, the application proceeds to check the neighborhood condition as follows: "IF there is more than 3 , 4 or 5 *Phragmites* cells surrounded , THEN the probability of growing reed is higher". In this research, the common reed grows in cell with 3 to 5 neighbors surrounded.

The following pseudo-code describes the alternative simplified function . Listing code 5.4 below initializes CA application in the beginning, then the algorithm reads data sources into system memory. Slope and elevation value are compared with those predefined values for common reed expansion, and number of reed-occupied cells are compared to the aforementioned neighborhood rule. By iterating this condition check for every cell within thee grid, the common reed coverage in the next generation or discrete time step is resulting.

```
1
2   INITIALISE CA application

4   BEGIN CA simulation iteration

6       Iterate through every cell FROM input raster layers
        /*  Standard deviation (SD)  */
8
            Choose a single cell N
10
          IF N.slope < MeanSlope + SlopeSD AND N.slope > MeanSlope-SlopeSD
12
                IF N.elevation < MeanElevation + ElevationSD AND
14                            N.elevation > MeanElevation - ElevationSD

16              IF N.reed.neighbours > Threshold number of neighborhood

18                    THEN N grow common reed in next time step

20          ELSE cell N does NOT grow reed in next time step

22  END of CA simulation iteration

24  Produce reed coverage map for next generation
```

Listing 5.4: Pseudo code for CA initialization subroutine

Chapter 6

Results and Discussion

This chapter demonstrates the results of the CA simulation model. The first scenario represents simulation result without condition constraints for *Phragmites* spreading. The second scenario defines a different type of neighborhood condition that enables *Phragmites* shrinking. The third simulation is developed from the previous 2 simulations; based on the comparison of simulation results, calibration can be made to facilitate the current CA simulation model.

6.1 Scenario of scratch

The simulation site is located in the Southern coastal area of Finland, near Porvoo area (see Figure 3.6).

6.1.1 Expanding

Scenario of scratch is the first scenario to demonstrate cellular automata simulation model. Scratch scenario operates without any constrain condition for plant growing, for instance no constrain is set to elevation, slope, nutrient or other factors. However, the neighborhood condition has to be defined to proceed with the simulation. The neighborhood condition is set as the following: IF there is more than 1 cell among 8 neighbors where common reed exists, $THEN$ the reed will expand to the cell in question in the next discrete time step.

The expanding scratch scenario starts from the common reed coverage in 2001(see Section 3.2.3). Year 2001 corresponds to generation "1" in the sim-

ulation model. Ten discrete time steps are generated to give the simulation results from 2001 to 2010. Figure 6.1 illustrates the results generated from this CA model:
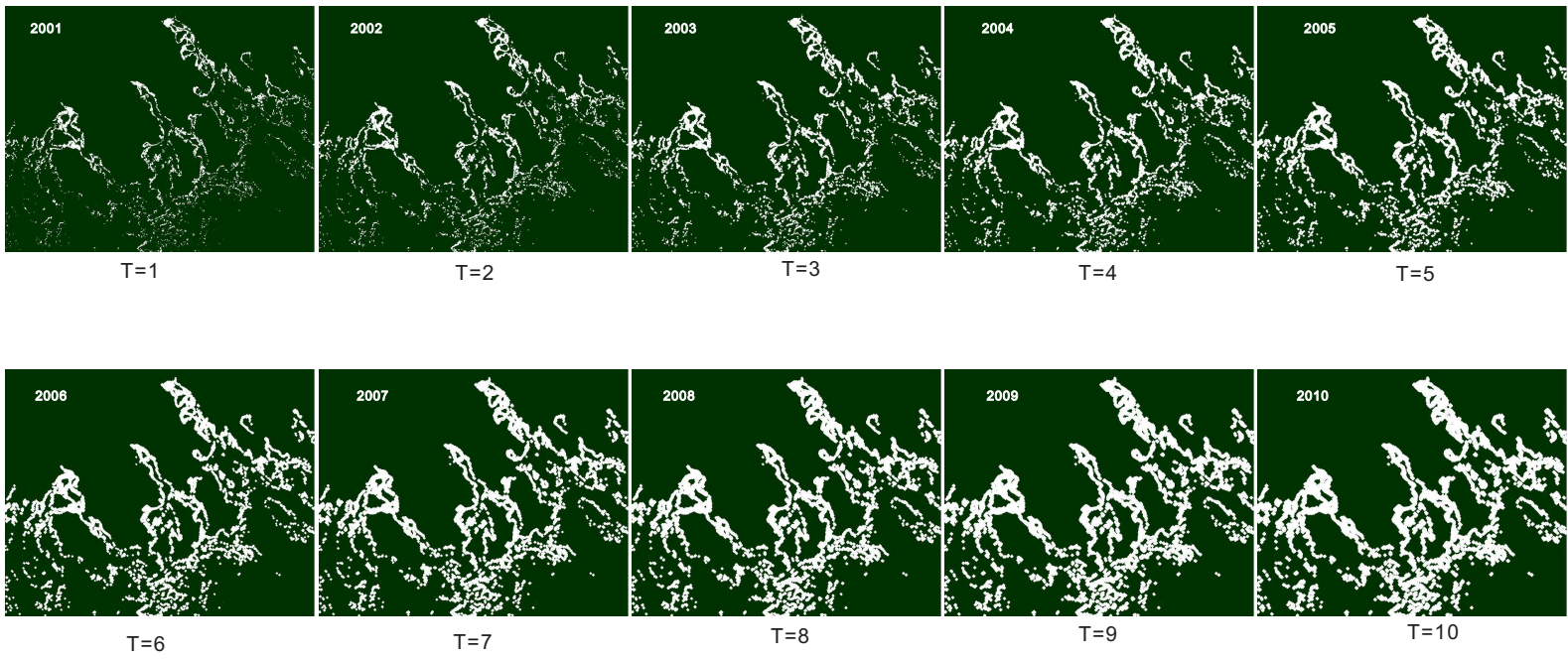
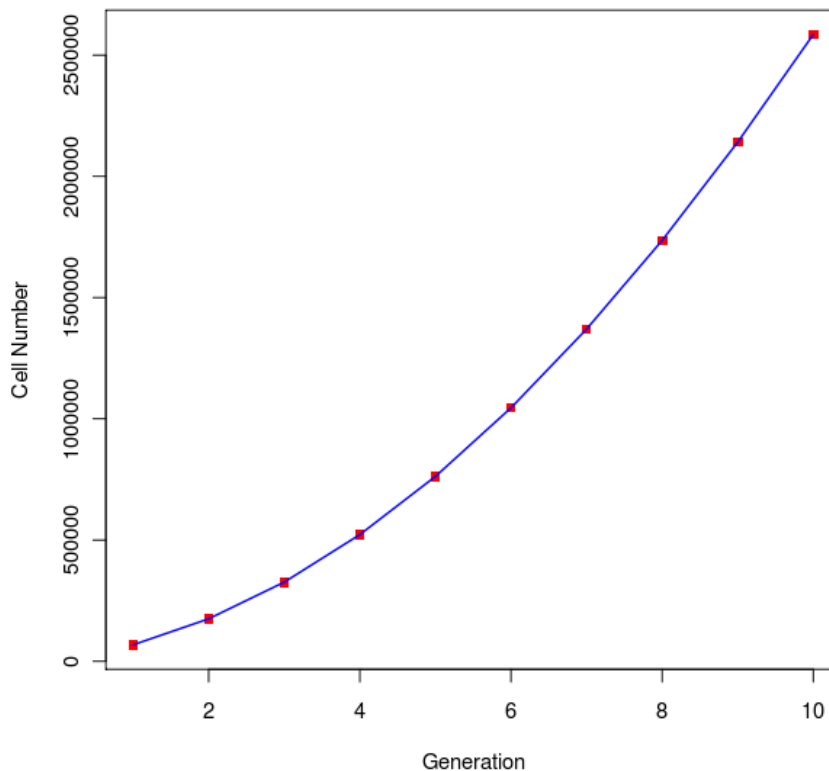Figure 6.1: Reed expanding from 2001 to 2010

Figure 6.2: Expanding speed graph

As a consequence of operating without constrained condition, Figure 6.1 illustrates a fiction simulation result: the common reed expands all over the area. The plant covers most of the coastal areas and heading towards the middle of the sea.

Phragmites australis cell numbers increase rapidly in expanding scenario (see Figure 6.2), empty cells are continuously occupied by the plant. Generation 1 is corresponding to year 2001 in expanding growing graph, generation 2 is corresponding to year 2002, and so forth. The coordinates origin represents number of cell occupied by plant in generation 1, which corresponds to 67748 cells. From generation 1 to 10 (year 2010), the cell number grows by 2517251. Average increment in cell number is 287222 per generation. Regression analysis reveals the cell growing trend is given by the equation $y=ax^2 + bx + c$. The equation is describing an accelerating expansion. The explanation is that the larger the plant coverage area contains more cells in

the edges, thus *Phragmites* expands faster in next generation.

6.1.2 Shrinking

Compared to the expansion simulation, shrinking is based on the fact that *Phragmites* has certain mortality rate which causes the shrinkage of common reed coverage. To simulate this shrinking process, the transition rule should be configured slightly different from the expansion simulation. While no rule is set to elevation, slope, nutrient and etc, the neighborhood control condition is set as: *IF* cell in question is not fully surrounded by reed, *THEN* the common reed in that cell will diminish in next discrete time step. This cab expressed as "cell on edges of the reed coverage will disperse in every new generation".

The shrinking scratch scenario starts from the original common reed coverage, year 2001, corresponding to discrete time step "1". It operates 10 generations, till year 2010; Figure 6.3 illustrates the results of this operation. Figure 6.3 also describes the shrinking simulation result: the plant shrinks continuously 10 years, and the coverage area decreases accordingly.

The common reed shrinking phenomenon demonstrates a trend of decrease in cell numbers (Figure 6.4). The raster map contains 67748 cells occupied by *Phragmites* in year 2001 (generation 1), this number decreases sharply in year 2002 to 59921 cells and gradually decline to 50422 in year 2010. The decline trend slowdown steadily in the next years, meanwhile the absolute decreased cell occupied by reed is decelerating. For instance from generation 1 to 2 the cell number drops down sharply by 7827, but this number is merely 3331 from generation 2 to 3. The cell number occupied by reed continues to fall till year 2010 and finally reaches 50422. Regression analysis of the shrink speed graph reveals the decline trend (see Figure 6.4) can be described by equation $y = ax^{-b} + c$. This equation reveals the shrinking is decelerating as number of generations grows. This the reed coverage area becomes smaller and less cells are therefore satisfying the mortality condition.

6.2 Scenario of optimal approximation

Unlike the scenario of scratch, optimal approximation scenario provides proper values and condition constraints for the common reed expanding phenomenon. The common reed is supposed to spread reasonably under these control conditions. Based on the available data sets and analysis results, the following
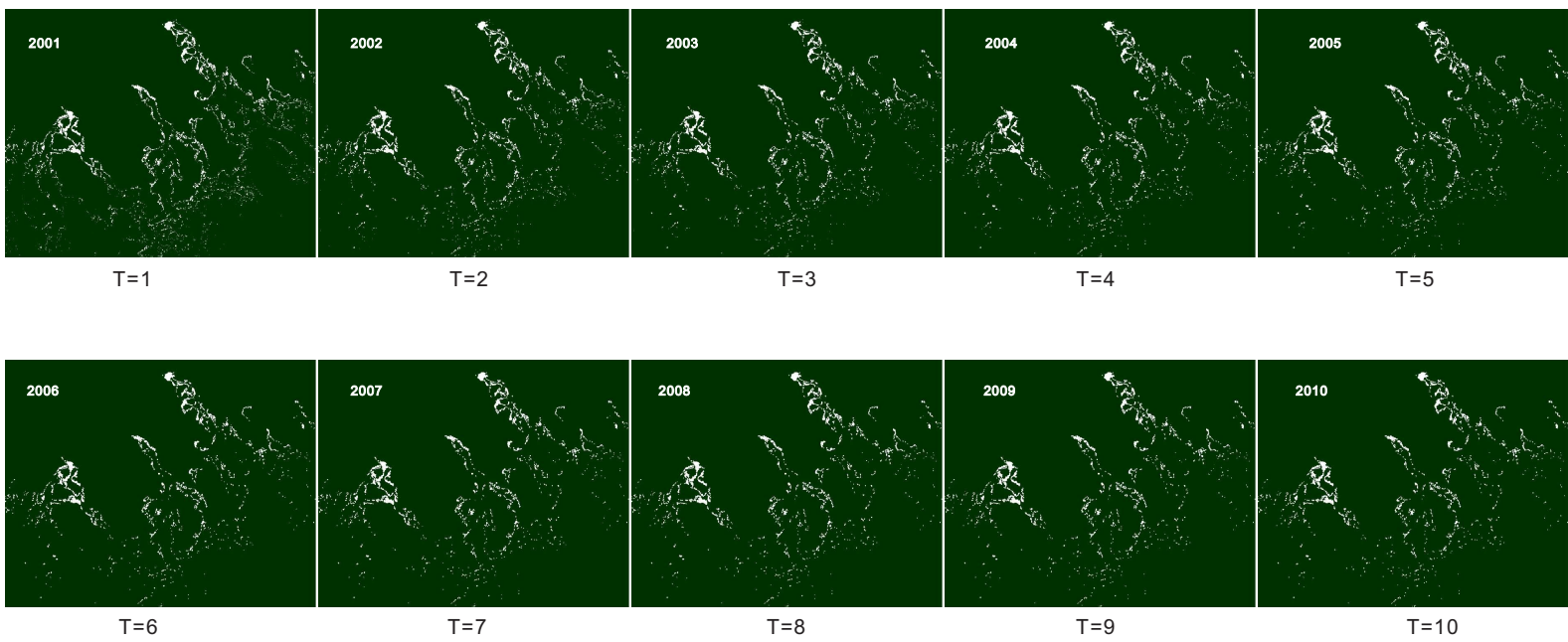
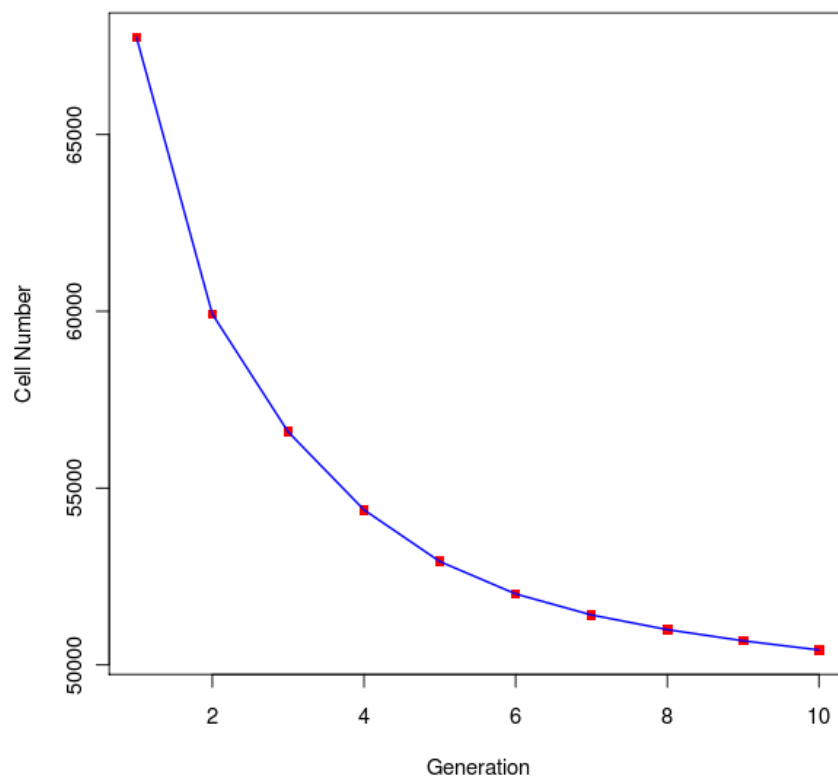Figure 6.3: Reed shrinking from 2001 to 2010

Figure 6.4: Shrinking speed graph

rules for CA simulation model are configured: elevation drops in the range of 2 standard deviation from the mean elevation value (see Figure 5.13), slope value drops in the range of 2 slope standard deviation from the slope mean (see Figure 5.13).

Besides the 2 condition constraints abovementioned, another influential constrainthood is the neighbor. In this optimal approximate operation, neighborhood threshold number is set to 4, that is, IF there are 4 cells occupied by reed around the current cell, $THEN$ common reed will expand to the cell in question in the next generation, $ELSE$ plant in the current cell shrink IF reed existed.

In addition, Monte Carlo method is included in the optimal simulation. Since uncertainty is associated with the common reed expansion phenomenon, by introducing Monte Carlo method, the simulation model can account for the randomness of the phenomenon. Monte Carlo method requires the simulation to run several times, thus simulation model can give eventually an optimal outcome. Figure 6.6 illustrates the simulation results after applying Monte Carlo method.
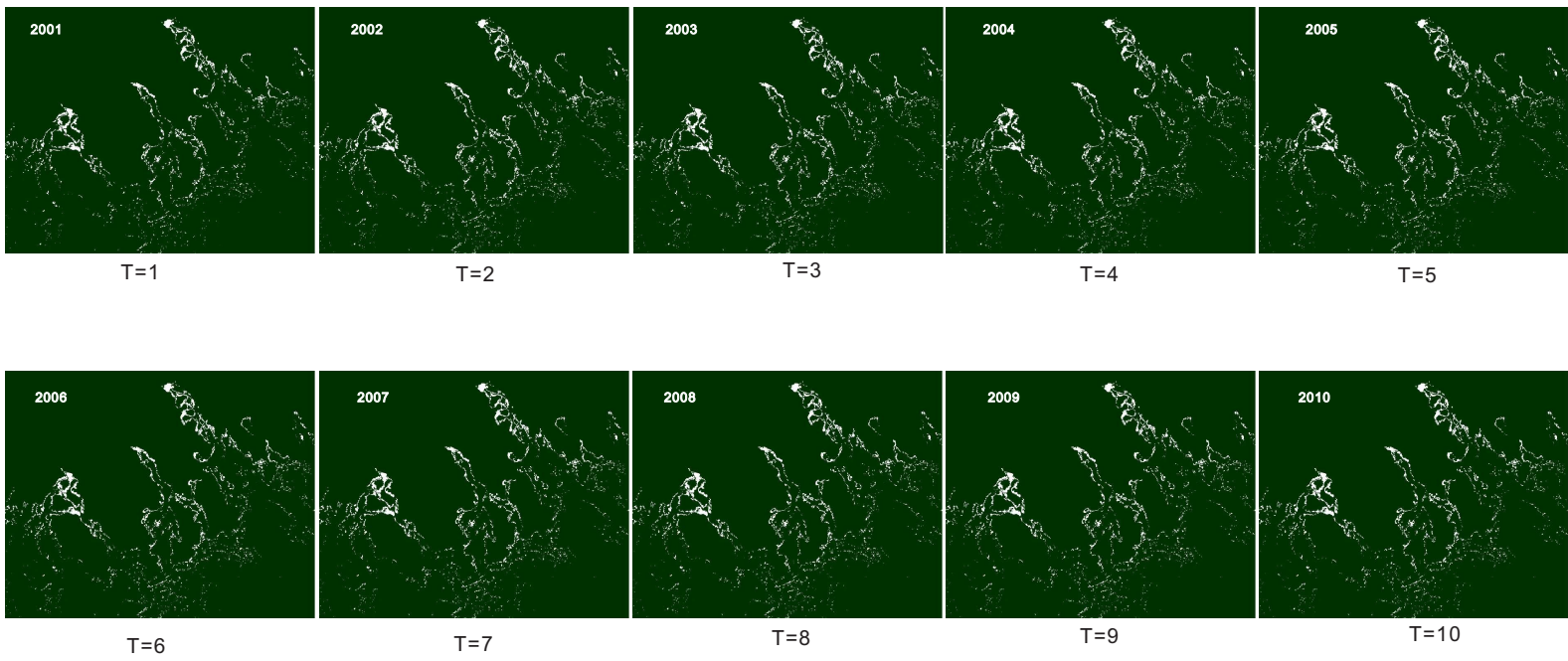
Figure 6.5: Optimal scenario of reed expanding from 2001 to 2010
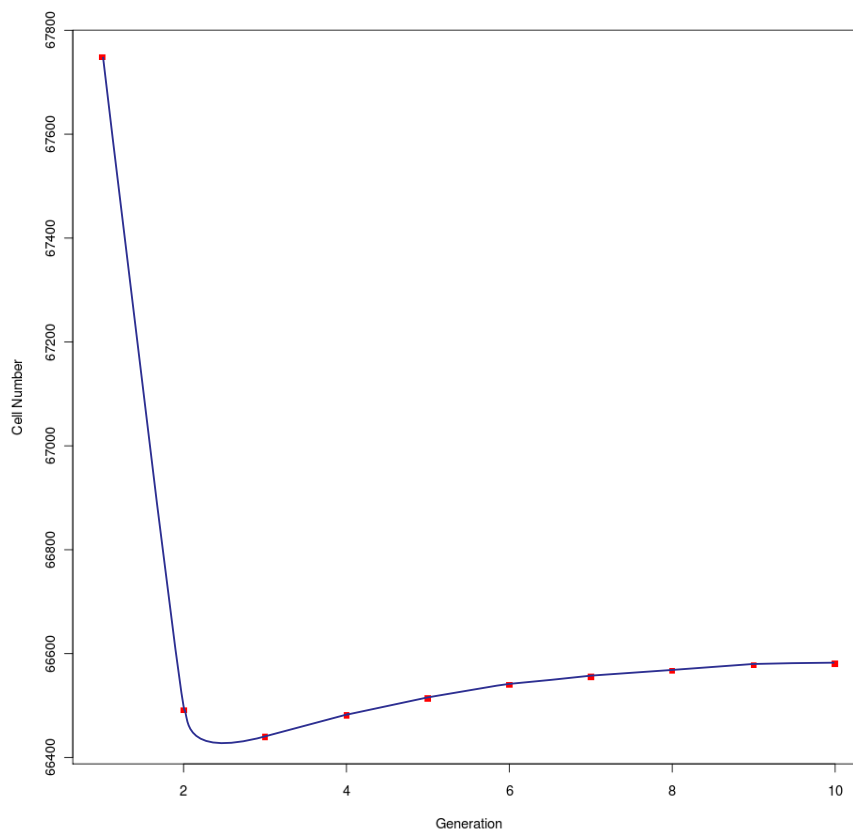
Figure 6.6: Optimal scenario graph

The simulation result of the optimal simulation is illustrated in Figure 6.5, the scenario is operated under proper configured conditions: the common reed grow in suitable water depth, shallow water areas with gentle slope seabed , and sufficient plant surroundings. This operation starts from generation 0 (year 2001) to generation 10 (year 2011). Compared with previous scratch scenarios, the expansion phenomenon becomes reasonable by predefined condition constraints. The common reed coverage expands in certain area; while the approximation also illustrates the plant can also shrink.

As shown in Figure 6.6, the expansion curve illustrates that the plant coverage area starts to shrink in the first few generations, and expand till steady afterwards. The cell number drops dramatically from 1st to 2nd generations, decreased by 1257 cells. Afterwards, it rises steadily during 2nd to 3rd generations, and increases smoothly from 4th to 8th generations. The cell numbers are fairly steady from generation 8th to 10th. Regression analysis concludes the curve can hardly be represents by a formula, since the growing curve represents duel decrement and incremental attributes. The optimal approximated growing curve represents best match phenomenon compared to plant expansion in reality.

Chapter 7

Conclusions and Limitations

7.1 Conclusions

The use of model factors and condition constraints influenced the model outcomes. Outcomes of scenario of scratch demonstrate abnormal and irregular results: *Phragmites* grows without any condition constraint, thus plant expands to cover most of the Finnish coast of the Gulf of Finland. The cause of this chaotic phenomenon is the scratch scenario does not include any factor and constrain condition, except the neighborhood condition.

The patterns acquired from the CA simulation results indicate the impact of spatial resolution. Changing of spatial resolution introduces significant variation in the simulation outcomes. The area occupied by reed decreases as data resolution increases. On the other hand, increasing the spatial resolution results in lowering the expansion speed.

Simulation outcomes vary significantly with different neighborhood conditions. Neighborhood conditions contribute to all simulation scenarios. The neighborhood rules are defined as: when the CA simulation model is expanding, the cell require less reed surrounding neighbors; when model is shrinking, it requires larger numbers of the reed surrounding; to satisfy both actions, neighborhood condition must be calibrated in a different mean.

Monte Carlo simulation method is introduced to solve the randomness of the phenomenon . Monte Carlo method turns the CA simulation model into an irreversible system, while originally CA modelse are reversible. The simulation model generates the same outcomes when Monte Carlo method is not applied. When applying Monte Carlo method, the CA model must be run several times to generate proper outcomes. Outcomes can be used

to construct a probability distribution graph, which reflects uncertainty and randomness.

To sum up, the following components have significant impact on the CA simulation model:

- Expansion suitability factors

- Spatial resolution (cell size)

- Neighborhood type and size

- Monte Carlo method

7.2 Limitations

Limitations in the CA simulation model cause certain imperfections in the simulation outcomes. Limited data sources as well as accuracy and uncertainty issues affect the CA simulation results. Limitations in data sources lead to further restriction in the analysis, which directly impact the determination of constrain factors. Data accuracy and uncertainty bring difficulties to the model validation, which is considered as a crucial stage to build the CA simulation framework. Moreover, instead of actual continuous time, discrete time step is applied in simulation model, which limits the model ability to simulate the phenomenon in reality.

Large amount of GIS data is required for realistic simulation. Data used in the current model were originated and acquired from several sources. For instance, the common reed coverage is obtained from a source different from some layers representing ecological factors, which were derived from the DEM. The accuracy of common reed coverage file is not defined and the data acquisition season is not certain. The common reed coverage varies in different seasons; plant coverage shrinks in the winter and expands in the summer as the temperature rises. Without enough knowledge about data acquisition time (season), the simulation time in CA model cannot be confirmed precisely. Similar problem exists in LiDAR data, which has less influence in simulation. DEM data for simulation model is combined from two sources with originally different spatial resolution. The coarse sea DDM had to be re-sampled to match the spatial resolution of the DEM on land. The re-sample process raises uncertainty issues in the simulation model. Furthermore, the analysis requires more detailed spatial resolution of DEM data, as

the resolution of the current DEM (25 X 25 meters) is considered coarse for such an application.

In addition, the lack of data regarding the ecological factors of the phenomenon has influenced the simulation results. Also, since the associated factors need to be analyzed both spatially and temporally, the lack of temporal data has negatively influenced the CA simulation model.

Unlike the actual continuous time, discrete time step is applied in CA simulation model. For *Phragimtes* expansion, one discrete time step equals to one year. Since common reed growing situation varies in different years, uncertainty of simulation rises as the discrete time or generations increases. For instance, because of the unexpected natural randomness, model outcomes can illustrate a realistic simulation in five discrete time steps but not in fifty steps. Therefore, discrete time in CA simulation model needs to be assessed accordingly.

Due to time limitation, the results from the simulation model were not validated. Validation can be used to determine the degree of correctness in representing the real world from the perspective of uses of model. Therefore the invalidated model has limited capability of predicting degree of accuracy and correctness for the real plant growing situation. Hence, further validation step can enhance the model credibility.

7.3   Recommendations

The current CA model establishes an acceptable simulation of *Phragimites* expansion. However, the model can be improved in several aspects. From the user point of view, it is preferable to have a Graphic User Interface (GUI). GUI can facilitate the usage of simulation program by easy means of configuration which makes it easier for end users. Moreover, in order to calibrate the probability calculation of the common reed expansion, Bayes theory can be introduced to the future model. Finally, further studies on model validation can be conducted in order to compare the model outcomes with the actual common reed coverage.

Bibliography

ABLE, K. AND HAGAN, S. 2000. Effects of common reed (phragmites australis) invasion on marsh surface macrofauna: Response of fishes and decapod crustaceans. *Estuaries 23*, 633–646.

ABLE, K. AND HAGAN, S. 2003. Impact of common reed, phragmites australis, on essential fish habitat: Influence on reproduction, embryological development, and larval abundance of mummichog (fundulus heteroclitus). *Estuaries 26*, 40–50.

ALT-EPPINGA, U., MIL-HOMENSB, M., AND HEBBELNA, D. 2007. Provenance of organic matter and nutrient conditions on a river- and upwelling influenced shelf: A case study from the portuguese margin. *Marine Geology 243*, 169–179.

ANDREW, M. E. AND USTINA, S. L. 2008. The role of environmental context in mapping invasive plants with hyperspectral image data. *Remote Sensing of Environment 112*, 4301–4317.

ANTONARAKIS, A., RICHARDS, K., AND BRASINGTON, J. 2008. Object-based land cover classification using airborne LiDAR. *Remote Sensing of Environment 112*, 2988–2998.

BART, D. AND HARTMAN, J. 2003. The role of large rhizome dispersal and low salinity windows in the establishment of common reed, phragmites australis, in Salt Marshes: New Links to Human Activities. *Estuaries 26*, 511–521.

BOLLIGER, J., SPROTT, J. C., AND MADENON, D. J. 2003. Self-organization and complexity in historical landscape patterns. *OIKOS 100*, 541–553.

BORK, E. W. AND SU, J. G. 2007. Integrating LiDAR data and multispectral imagery for enhanced classification of rangeland vegetation: A meta analysis. *Remote Sensing of Environment 111*, 11–24.

Brennan, R. and Webster, T. 2006. Object-oriented land cover classification of LiDAR-derived surfaces. *Can. J. Remote Sensing 32*, 162–172.

Burdick, D. M. and Konisky, R. A. 2003. Determinants of expansion for Phragmites australis, Common Reed, in Natural and Impacted Coastal Marshes. *Estuaries 26*, 407–416.

Clarka, M. L., Robertsa, D. A., and Clarkb, D. B. 2005. Hyperspectral discrimination of tropical rain forest tree species at leaf to crown scales. *Remote Sensing of Environment 96*, 375–398.

Colasanti, R., Hunt, R., and Watrud, L. 2007. A simple cellular automaton model for high-level vegetation dynamics. *Ecological Modelling 203*, 353–374.

Dickie, S. 2001. Application of Airborne Scanning LiDAR to Forestry: Examining Stand Height and Crown Closure in Annapolis County, Nova Scotia. Tech. rep., Applied Geomatics Research Group, Centre of Geographic Sciences(COGS).

Doody, J. S., Sims, R. A., and Letnica, M. 2007. Environmental manipulation to avoid a unique predator: Drinking hole excavation in the agile wallaby, macropus agilis. *Ethology 133*, 128–136.

E. Minchinton, T. 2002. Precipitation during El Niño correlates with increasing spread of phragmites australis in New England, USA, coastal marshes. *MARINE ECOLOGY PROGRESS SERIES 242*, 305–309.

Ekebom, J., Laihonen, P., and Suominen, T. 2003. A GIS-based stepwise procedure for assessing physical exposure in fragmented archipelagos. *Estuarine, Coastal and Shelf Science 57*, 887–898.

Fonstad, M. A. 2006. Cellular automata as analysis and synthesis engines at the geomorphology ecology interface. *Geomorphology 77*, 127–234.

Gardner, M. 1970. Mathematical games the fantastic combinations of john conway's new solitaire game.

Gewin, V. 2005. Industry lured by the gains of going green. *Nature 437*, 14.

Goodchild, S. 2006. *Geospatial Analysis - a comprehensive guide*. Longley. http://www.spatialanalysisonline.com/OUTPUT/html/CellularautomataCA.html.

GUCKER, C. L. 2010. Phragmites australis. Fire Effects Information System. `http://www.fs.fed.us/database`.

HARRI TOLVANEN, T. S. 2005. Quantification of openness and wave activity in archipelago environments. *Estuarine, Coastal and Shelf Science 64*, 436–446.

HASLAM, S. 1972. Biological flora of the british isles. phragmites communis trin. *Journal of Ecology 60*, 585–610.

HAVENS, K. J., BERQUIST, H., AND PRIEST, W. I. 2003. Common Reed Grass, Phragmites australis, Expansion into Constructed Wetlands: Are We Mortgaging Our Wetland Future. *Estuaries 26*, 417–422.

HAYBALL, N. AND PEARCE, M. 2004. Influences of simulated grazing and water-depth on the growth of juvenile bolboschoenus caldwellii, phragmites australis and schoenoplectus validus plants. *Aquatic Botany 78*, 233–242.

IKONEN, I. AND HAGELBERG, E. 2007. Read up on reed! end report of the reed strategy -project (interreg iiia programme). Tech. rep., Southwest Finland Regional Environment Centre.

JACQUEMOUD, S. AND BARET, F. 1990. Prospect: A model of leaf optical properties spectrastar. *Remote Sensing of Environment 34*, 75–91.

JANSSENS, K. 2009. An introductory review of cellular automata modeling of moving grain previous boundaries in polycrystalline materials. *Mathematics and Computers in Simulation*.

JARVIS, J. D., BROWN, R. G., AND SPITTLE, A. J. 2000. Modelling of non-equilibrium solidification in ternary alloys : Comparison of 1d, 2d, and 3d cellular automaton-finite difference simulations. *Materials science and technology 16*, 1239–1436.

JEPSON, W. AND HICKMAN, J. 1993. *The Jepson manual: higher plants of California*. University of California Press, 1282,1285.

KIVIAT, E. AND HAMILTON, E. 2001. Phragmites use by native north americans. *Aquatic Botany 69*, 341–357.

KOETZ, B., MORSDORF, F., VAN DE LINDEN, S., CURT, T., AND ALLGOWER, B. 2008. Multi-source land cover classification for forest fire management based on imageing spectrometry and LiDAR data. *Forest Ecology and Management 256*, 263–271.

Kronholm, K. and Birkeland, K. W. 2004. Integrating spatial patterns into a snow avalanche cellular automata model. Tech. rep., Department of Earth Sciences, Montana State University.

Lee Ellis, S. 2005. The establishment, expansion and ecosystem effects of Phragmites australis, an invasive species in coastal Louisiana. M.S. thesis, INNOVATION UNIVERSITY.

Lelong, B., Lavoie, C., and Jodoin, C. 2007. Expansion pathways of the exotic common reed (phragmites australis): a historical and genetic analysis. *Diversity and Distributions 13*, 430–437.

Mack, R. N. and Lonsdale, W. M. 2002. Eradicating invasive plants: Hard-won lessons for islands. *Invasive Species Specialty*.

Mack, R. N., Simberloff, D., Lonsdale, W. M., Evans, H., Clout, M., and Bazzaz, F. 2000. Biotic invasions: Causes, epidemiology, global consequences, and control. *Ecological Applications 10*, 689–710.

Mcgaughey, B. and Reutebuch, S. 2009. Getting Started with FUSION. Website. `http://forsys.cfr.washington.edu/fusion.html`.

Mooney, H. A., Cropper, A., and Capistrano, D. 2005. Millennium Ecosystem Assessment:ecosystems and human well-being: Biodiversity Synthesis. Tech. rep., World Resources Institute.

Pitkanen, T. 2006. Missa ruokoa kasvaa? jarviruokoalueiden satelliittikartoitus etela-suomen ja viron vainameren rannikoilla. *Turun ammattikorkeakoulun puheenvuoroja(Finnish language) 29*, 82.

Raichel, D., Able, K., and Hartman, J. 2003. The influence of phragmites (common reed) on the abundance, and potential prey of a resident marsh hackensack meadowlands, new jersey. *Estuaries 26*, 511–521.

R.Bodensteiner, L. and O.Gabriel, A. 2003. Response of mid-water common reed stands to water level variations and winter conditions in Lake Poygon, Wisconsin, USA. *Aquatic Botany 76*, 49–64.

Rickey, M. A. and Anderson, R. C. 2004. Effects of nitrogen addition on the invasive grass phragmites australis and a native competitor spartina pectinata. *Journal of Applied Ecology 41*, 888–896.

R.Minkoff, D., Escapa, M., E.Ferramola, F., D.Maraschn, S., O.Pierini, J., M.E.Perillo, G., and Delrieux, C. 1992. Effects of

crabchalophytic plant interactions on creek growth in a s.w. atlantic salt marsh: A cellular automata model. *Water Resoure 28*, 2183–2195.

SALTONSTALL, K. 2006. Phragmites australis (grass). Global Invasive Species Database. `http://www.issg.org/database/species`.

SALTONSTALL, K. AND STEVENSONA, J. C. 2007. The effect of nutrients on seedling growth of native and introduced phragmites australis. *Aquatic Botany 69*, 341–357.

STAFFEN, A., REINARTZ, J., AND BOOS, T. 2003. Invasive plants of wisconsin. Tech. rep., Invasive Plants Association of Wisconsin.

TOFFOLIA, T. 1984. Cellular automata as an alternative to (rather than an approximation of) differential equations in modeling physicsstar. *Physica D: Nonlinear Phenomena 10*, 117–127.

UNDERWOOD, E., USTIN, S., AND DIPIETRO, D. 2003. Mapping nonnative plants using hyperspectral imagery. *Remote Sensing of Environment 86*, 150–161.

VAN DER PUTTEN, W. H. 1998. Die-back of phragmites australis in european wetlands: an overview of the european research programme on reed dieback and progression. *Aquatic Botany 59*, 263–275.

WEBSTER, T. L., MURPHY, J. B., AND GOSSE, J. C. 2006. Mapping subtle structures with light detection and ranging(LiDAR): flow units and phreatomagmatic rootless cones in the north mountain basalt, nova scotia. *Can. J. Earth Science 43*, 157–176.

WEINSTEIN, M. P. AND BALLETTO, J. H. 1999. Does the common reed , phragmites australis, affect essential fish habitat? *Estuaries 22*, 793–802.

WOLFRAM, S. 1984. Universality and complexity in cellular automata. *Physica D: Nonlinear Phenomena 10*, 1–35.

WOLFRAM, S. 1986. Random sequence generation by cellular automata. *Advances in Applied Mathematics 7*, 123–169.

WOLFRAM, S. 2002. *A New Kind of Science*. Wolfram Media, Champaign, IL, 71, 876.

YACOUBI, S. E. AND JAI, A. E. 2002. Cellular automata modelling and spreadability. *Mathematical and Computer Modelling 36*, 1959–1074.

Zhang, Y., Pulliainen, J., Koponen, S., and Hallikainen, M. 2005. Water quality retrievals from combined landsat tm data and ers-2 sar data in the gulf of finland. *IEEE Transactions on Geoscience and Remote Sensing 41*, 622–629.